การศึกษาผลกระทบของความดันก๊าซ ต่อการยกตัวของอนุภาคทรงกลมภายใต้สนามไฟฟ้า

นายหมอนคำ วิไลเซียน

วิทยานิพนธ์นี้เป็นส่วนหนึ่งของการศึกษาตามหลักสูตรปริญญาวิศวกรรมศาสตรมหาบัณฑิต
สาขาวิชาวิศวกรรมไฟฟ้า ภาควิชาวิศวกรรมไฟฟ้า
คณะวิศวกรรมศาสตร์ จุฬาลงกรณ์มหาวิทยาลัย
ปีการศึกษา 2559

Study on the Effects of Gas Pressure on the Liftoff of Spherical Particles under Electri c field

Mr. Monekham Vilaisien

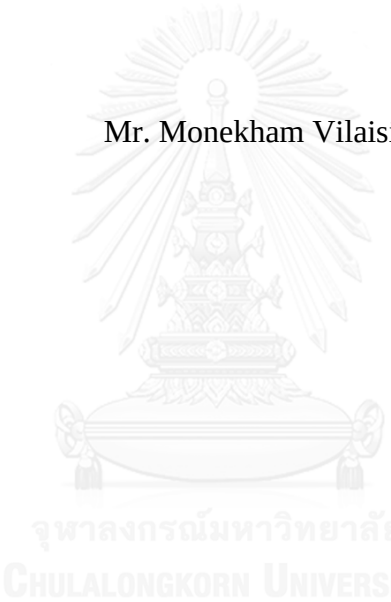

A Thesis Submitted in Partial Fulfillment of the Requirements
for the Degree of Master of Engineering Program in Electrical Engineering
Department of Electrical Engineering
Faculty of Engineering
Chulalongkorn University
Academic Year 2016

Thesis Title	Study on the Effects of Gas Pressure on the Liftoff of Spherical Particles under Electric field
By	Mr. Monekham Vilaisien
Field of Study	Electrical Engineering
Thesis Advisor	Professor Boonchai Techaumnat, Ph.D.

Accepted by the Faculty of Engineering, Chulalongkorn University in Partial Fulfillment of the Requirements for the Master's Degree

.....Dean of the Faculty of Engineering
(Associate Professor Supot Teachavorasinskun, Ph.D.)

THESIS COMMITTEE

.....Chairman
(Assistant Professor Komson Petcharaks, Ph.D.)
.....Thesis Advisor
(Professor Boonchai Techaumnat, Ph.D.)
.....External Examiner
(Nutthaphong Tanthanuch, Ph.D.)

หมอนคำ วิไลเซียน : การศึกษาผลกระทบของความดันก๊าซ ต่อการยกตัวของอนุภาคทรงกลมภายใต้สนามไฟฟ้า (Study on the Effects of Gas Pressure on the Liftoff of Spherical Particles under Electric field) อ.ที่ปรึกษาวิทยานิพนธ์หลัก: บุญชัย เตชะอำนาจ, 55 หน้า.

ระบบสวิตช์เกียร์แบบฉนวนก๊าซถูกใช้เป็นส่วนใหญ่ในสถานีไฟฟ้าแรงสูง เนื่องจากระบบดังกล่าวสามารถติดตั้งในบริเวณที่มีพื้นที่จำกัดได้, ต้องการการบำรุงรักษาต่ำ, มีความน่าเชื่อถือ และ ความปลอดภัยสูง. สาเหตุความบกพร่องที่เกิดขึ้นกับระบบสวิตช์เกียร์แบบฉนวนก๊าซส่วนใหญ่มาจากการปนเปื้อนของอนุภาคตัวนำในภายในระบบ. วิทยานิพนธ์นี้ ได้ศึกษาสนามไฟฟ้ายกตัวของอนุภาคทรงกลมตัวนำที่อยู่ระหว่างอิเล็กโตรดขนาน โดยทำการทดลองภายใต้เงื่อนไขความดันและชนิดของก๊าซที่แตกต่างกัน. ระยะห่างระหว่างอิเล็กโตรดเท่ากับ 10 มิลลิเมตร. อนุภาคทรงกลมที่ใช้ในการทดลองเป็นอลูมิเนียมรัศมีเท่ากับ 0.4, 0.68 และ 1 มิลลิเมตร เหล็กรัศมีเท่ากับ 0.5 มิลลิเมตร และ สเตนเลสรัศมีเท่ากับ 1 มิลลิเมตร. สำหรับการทดลองที่ใช้อากาศเพียงอย่างเดียวใช้ความดันเท่ากับ 0.5, 0.75, 1, 2 และ 3 บาร์ ส่วนการทดลองที่ใช้อากาศผสมกับก๊าซซัลเฟอร์เฮกซาฟลูออไรด์และการทดลองที่ใช้อากาศผสมกับก๊าซไนโตรเจนใช้ความดันเท่ากับ 1 และ 3 บาร์. ก๊าซผสมมีอัตราส่วนเท่ากับ 1:1. ผลการทดลองแสดงให้เห็นว่าการยกตัวของอนุภาคขึ้นอยู่กับความดันของก๊าซและขนาดของอนุภาค เนื่องจากสนามไฟฟ้ายกตัวเพิ่มขึ้นอย่างมีนัยสำคัญเมื่อความดันก๊าซและขนาดอนุภาคเพิ่มขึ้น. นอกจากนั้น สนามไฟฟ้ายกตัวในกรณีของก๊าซผสมมีค่าน้อยกว่าสนามไฟฟ้ายกตัวในกรณีที่ใช้อากาศเพียงอย่างเดียว. ความแตกต่างของสนามไฟฟ้ายกตัวระหว่างแรงดันขั้วบวกกับแรงดันขั้วลบเห็นได้อย่างชัดเจนในกรณีของอากาศที่ความดันก๊าซมีค่าเท่ากับ 3 บาร์ หรืออนุภาคที่มีรัศมี 0.4 มิลลิเมตร. ในกรณีที่ใช้ก๊าซผสมพบว่าขั้วแรงดันมีผลต่อสนามไฟฟ้ายกตัวของอนุภาคลดลงอย่างมีนัยสำคัญ. ความแตกต่างของแรงไฟฟ้าสถิตและแรงโน้มถ่วงมีค่าเพิ่มขึ้นสัมพันธ์กับพื้นที่ผิวของอนุภาคและความดันก๊าซในลักษณะเชิงเส้น. ทั้งนี้ ความแตกต่างของแรงทั้งสอง ในกรณีที่ใช้ตัวกลางเป็นก๊าซผสมมีค่าน้อยกว่าการใช้อากาศเพียงอย่างเดียว.

ภาควิชา วิศวกรรมไฟฟ้า ลายมือชื่อนิสิต .....

สาขาวิชา วิศวกรรมไฟฟ้า ลายมือชื่อ อ.ที่ปรึกษาหลัก .....

ปีการศึกษา 2559

5770525721 : MAJOR ELECTRICAL ENGINEERING
KEYWORDS: GAS INSULATED SYSTEM / GAS PRESSURE / LIFTINF ELECTRIC FIELD / PARTICLE

MONEKHAM VILAISIEN: Study on the Effects of Gas Pressure on the Liftoff of Spherical Particles under Electric field. ADVISOR: PROF. BOONCHAI TECHAUMNAT, Ph.D., 55 pp.

The gas insulated switchgears are widely used in high voltage substation due to their advantages, such as smaller space requirement, less frequent requirement for maintenance, high operational reliability and safety. The failures in gas insulated switchgears due to the contamination of conducting particles are critical. This thesis studied the experiments on the lifting electric field of spherical particles under different gas types and pressures between parallel electrodes. The electrode gap was 10 mm. The various materials and sizes of spherical particles were used. The particle radius was 0.4, 0.68 and 1.19 mm for aluminum, 0. 5 mm for steel, and 1 mm for stainless steel spheres. We carried out the experiments under pressures of 0.5, 0.75, 1, 2 and 3 bar for the air, and 1 and 3 bar for a mixture of air/SF_6 and air/N_2. The proportion of gas mixtures was 1:1. The experimental results indicated that the particle liftoff depended on the pressure and the particle size for all gas media. The lifting electric field increased significantly with increasing the pressures and particle sizes. In addition, the lifting electric field of particle liftoff in the gas mixtures was smaller than that in the air under same pressure for each particle size. The difference in lifting electric field from positive and negative voltage was clear under 3 bar pressure or the particle of 0.4 mm radius in the air. However, the case of the gas mixtures indicated that the difference in the lifting electric field was significantly reduced. The difference between the electrostatic force and the gravitational force increased approximately by a linear relationship with the product of particle surface area and gas pressure. The force difference of the gas mixtures was smaller than that of the air.

Department: Electrical Engineering Student's Signature .....
Field of Study: Electrical Engineering Advisor's Signature .....
Academic Year: 2016

ACKNOWLEDGEMENTS

This work was supported by the AUN/SEED-Net program, JICA, and the Thailand Research Fund. The authors want to thank Prof. Kunihiko Hidaka, The University of Tokyo, for his help and discussion on the experiments. The authors sincerely acknowledge Tatchawin Sangsri, Teera Kriengkriwut, Chomrong Ou, Nitipong Panklang and Sinthanou Konglysan for their helps in my experiments. I thank Thavorn Auedee and Kriengkrai Odthanu for providing knowledge and training related to high voltage equipment and their systems, which are important for my thesis.

CONTENTS

Page

LIST OF TABLES

LIST OF FIGURES

CHAPTER 1
INTRODUCTION

1.1 Overview of gas insulated systems

Nowadays, the population and industrial sectors are growing significantly. As a consequence, the demand for electric power is increasing. High voltage substations increase significantly to meet the power demand. Normally, there are many types of insulation systems used in substations including air and gas insulated systems. The air insulated systems are low cost, but need large area to accommodate required dielectric strength. Therefore, they are inappropriate for areas of the dense population, particularly large cities due to valuable space. Hence, the gas insulated systems are a possible alternative for the urban areas due to their advantages over the air insulated systems [1, 2], such as smaller space requirement, no effect of environmental condition on the insulation system, less frequent requirement for maintenance, high operational reliability and safety. The gas insulated systems include gas insulated switchgears (GIS), gas insulated transmission lines and gas insulated transformers.

GIS are one of the most important apparatus in high voltage substations. The sulfur hexafluoride (SF_6) is the typical gas in GIS due to the high insulation strength. The functional elements of GIS are the same as air insulated switchgear. The main structures of GIS are high voltage conductor, metal enclosure and gas insulation [3]. The gas inside of a GIS has a pressure in a range between 3 and 7 bar [2] because the dielectric strength of gas depends on the gas density and increases by using higher pressure [4]. Therefore, the pressure inside of the GIS is a major factor for yielding sufficient dielectric strength, which increases operation reliability, safety and space reduction.

It is well known that one of the major failure causes of GIS is the existence of free particles in the gas. They possibly cause corona discharge and complete breakdown in the insulation systems [5, 6]. The degree of severity depends on a variety of factors such as particle shape, size, material, level of the applied electric field and gas pressure. The most likely causes of particle contamination are the fabrication, assembly, or maintenance processes as well as the switching operation. In practical systems, it is

very difficult to avoid free particle contamination in the GIS. The sizes of particles in actual GIS are mostly smaller than 0.5 mm [7]. However, sometimes particles larger than 1 mm are also found. The particles have the difference in the geometrical shape and material, and can be classified as conductor and dielectric ones. The movement of conducting particles is much simpler than that of dielectric ones. The particles can move freely within the GIS under high electric field [8]. Their motion can reduce the insulating capability of the gas insulated system, making the loss of gas dielectric strength in GIS due to the particle contamination more serious [9].

This thesis studies the liftoff of conducting particle under different gas pressures. The main objective of the study is to clarify the effect of the gas pressure on the critical field for the liftoff in relation with the particle size and materials involved.

1.2 Literature review

Previously, there are several studies on the movement behavior of the particles in the insulation system and on the fundamentals of particle deactivation.

K. Sakai et. al. studied the conducting particle motion and particle-initiated breakdown in non-uniform electric field [10]. The stainless steel sphere and aluminum needle-shaped particles were used. The radius of spherical particle was 1 mm. The diameter of needle-shaped particle was 1 mm and the length was 3 mm. The motion of the spherical particle was estimated by experiments and by solving the motion equation numerically. The experiments were conducted in atmospheric air. The non-parallel electrode plates were used. The experiments and estimations showed that the initial particle motion was strongly influenced by the electric field condition around the particle. The particle moved to the higher electric field region by effect of the electrical gradient force and Coulomb force. The particle in the higher electric field region caused the breakdown of the gap. It was found that the breakdown voltage of the gap was decreased by the effect of the microdischarges between the particle and electrode.

K. Sakai et. al. studied the spherical conducting particle behavior between non-parallel plane electrodes in atmospheric air [11]. The angle between the planes was 3.5º. The particle behavior was investigated theoretically and experimentally under AC voltage with various frequencies. Stainless steel spherical particles were used. The radius of the particles was 0.25, 0.5 and 1 mm. The results of study showed that the

particles moved along the grounded electrode toward the higher electric field region by the action of the electrical gradient force and then lifted from the electrode.

K. Sakai et. al. studied the motion of wire particle in non-uniform electric field [12]. Experiments were used to investigate the particle behavior between the non-parallel plane electrodes. The angle between the planes was 3.5^{o}. The DC positive or negative voltage was applied to the electrode system. The diameter of aluminum wire particle was 0.25 mm and the length was 3 mm. The results showed that when corona discharge was maintained at the end of the wire particle, the particle tended to stand on a negatively charged electrode. The particle moved laterally toward decreasing electrode gap regions by the electrical gradient force. The particle-triggered breakdown occurred at high field regions.

K. Sakai et. al. studied the wire particle behavior in the non-uniform AC electric field [8]. The experiments were conducted in atmospheric air. The non-parallel plane electrode system was used. The diameter of stainless steel and aluminum wire particles was 0.5 mm and the length was 2 mm. The results showed that the particles traveled into the high electric field regions regardless of the corona discharge. When microdischarges occurred between the particles and electrode, the particle-triggered breakdown voltage decreased.

K. Sakai et. al. investigated the free conducting particle behavior and particle charging on a coated electrode in non-uniform DC and AC electric fields [13]. The experiments were mainly carried out by using non-parallel plane electrode system. The grounded electrode was covered with a dielectric of 50 μm thickness. The applied voltage was positive DC, negative DC or 60 Hz AC. The stainless steel sphere of 1 mm radius was used. The results of the study showed that the particle can be charged through partial discharges between the particle and coating. In addition, the particle moved laterally on the coated electrode toward increasing electric field regions by the action of the electrical gradient force, which was independent of the charge on the particle.

N. Phansiri et. al. studied the electromechanics of a conducting particle under non-uniform electric field [14]. The objective was to investigate the feasibility of particle manipulation by the dielectrophoretic (DEP) force for insulation systems. The experimental results were compared with the simulation results. The non-parallel plate

electrodes with the tilt angle of 3° and 15° were used. The lower electrode was grounded, and the high voltage was applied to the upper electrode. The aluminum and stainless steel spheres of 0.4 mm radius were placed on the grounded electrode. For the experiments, the grounded electrode was coated by dielectric layers of 1 mm thickness. The results showed that the particle was moved to the higher field region by the DEP force and immobilized at the termination of the dielectric layers. In the cases of the particle behavior without dielectric coating, the particle moved to the region of lower electric field, and the lateral displacement increased with the tilt angle between the electrodes.

V. Q. Huynh studied the movement of the non-spherical particles under electric field in dielectric system [7]. He carried out analytical and experimental studies on the electromechanics of non-spherical particles under electric field. Two parallel electrodes were used. The gap between the electrodes was 9, 10 and 18 mm. The experiments were conducted mostly in atmospheric air. In some case, the pressure was 2 bar. The aluminum prolate spheroidal and wire particles with different ending profiles were used. The length of the prolate spheroidal particles was 4 mm and minor axes were 1 and 2 mm for the small and large particles, respectively. The diameter of the wire particle was 0.5 mm and the length was 2 and 4 mm. The results showed that the lifting electric field and movement of particle did not only depend on the electrode gap and particle size for the spheroidal particle because most of the particle movements were moved initially at the end and then lifted from the lower electrode. On the cases of wire particles, the lifting electric field was depended on the ending profile and orientation of the particles on the grounded electrode. The particle movement was moved initially at end of stronger field.

H. Parekh et. al. studied the lifting field of free conducting particles in compressed SF_6 gas with dielectric coated electrodes [15]. The objective was to investigate the physical mechanisms responsible for the acquisition of charge by the particles. The theoretically calculated results were compared to experimental results. The experiments were done under the uniform electric field in the SF_6 gas at pressures up to 6.8 bar. The aluminum electrode gap was 1.5 cm. The lower electrode was coated by dielectrics. The thickness of the dielectric coating was varied from 5 to 115 μm. The spherical particles of copper and steel were used. The diameters of the spherical

particles were varied from 1 mm to 3 mm. A computer program was used to calculate the electric field in the vicinity of the particle. The results of the study showed that the partial discharges between particle and dielectric coated electrode took place at sufficiently high values of electric field. At higher gas pressures, higher electric fields were necessary for the partial discharges to take place. A particle also acquired charges from a conductive charge transport through the dielectric coating. Charging particle through dielectric material was clearly independent of the pressure of the gas.

The aforementioned research works show that the only the effects of electrostatic and gravitational force on particle motion are usually considered in the analysis. The effects of polarity voltage and particle sizes for case of varied pressures have not been presented. Gas pressure may be an additional factor affecting the motion inception of particles. Therefore, this thesis studies the effects of gas pressure on the liftoff of conducting particle in the uniform DC electric field under air and SF_6 gas pressure. The experiments and analysis will be used to find the lifting electric field of the liftoff of particles. The effect of pressure can be analyzed from consideration of the lifting electric field. In order to generalize our findings, different sizes and particle materials are used. In addition, this work also varies the gas medium.

1.3 Objectives of dissertation

1 To study experimentally the lifting electric field of the conducting particles

2 To analyze the effects of voltage polarity, particle size and gas pressure on the liftoff of the conducting particles

1.4 Expected results

The effects on conducting spherical particle liftoff are expected to be clarified from the study. The results of this work can be useful for particle deactivation in practice where pressurized conditions of gas media are typical.

1.5 Scope of dissertation

5.1 Study in the uniform electric field under DC voltage

5.2 Consider only conducting spherical particle

5.3 The gaseous media are the air and gas mixture of air and SF_6 or air and N_2. The proportions of gas mixture are 1:1.

CHAPTER 2
THEORETICAL BACKGROUND

2.1 Liftoff of spherical particle

Consider an electrode system of two parallel plates, as shown in Figure 2.1. The electric field is uniform. The lower electrode is grounded. The upper electrode is connected to a DC high voltage. A conducting particle is on the ground electrode under electric field E_0. The particle can be lifted from ground electrode when the electrostatic force F_e overcomes the particle weight W, pressure force and adhesion force F_{ad}. For the parallel electrodes, the particle moves vertically between lower and upper electrodes. When the particle touches an electrode, a charge transfer takes place.

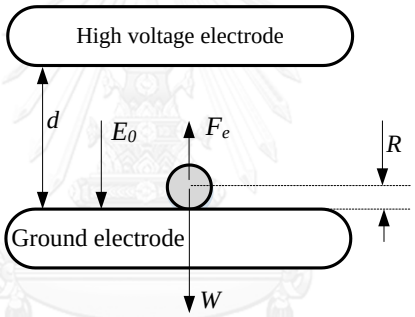

Figure 2. 1. Particle lying in the parallel-plate electrode system.

2.1.1 Induced charge

Consider a conducting spherical particle of radius R placed on the ground electrode under electric field E_0. It will acquire a charge Q given by [7]

$$Q = \frac{2}{3}\pi^3 \varepsilon_E R^2 E_0 \tag{2.1}$$

where ε_E is the permittivity of the medium. $\varepsilon_E = \varepsilon_0$ (8.854×10^{-12} F/m) for the air and other gases.

2.1.2 Electrostatic force on particle

The electrostatic force F_e on the charge Q in a uniform electric field E_0 can be determined as [14]

$$F_e = 0.832 Q E_0 \tag{2.2}$$

The surface area of sphere is $S = 4\pi R^2$. The induced charge can be written as

$$Q = 1.645\varepsilon_E SE_0 \tag{2.3}$$

and

$$F_e = 1.369\varepsilon_E SE_0^2 \tag{2.4}$$

2.1.3 Particle weight

Particle weight is a function of the material and volume of the particle. The weight of a spherical particle is

$$W = \frac{4}{3}\pi R^3 \rho g \tag{2.5}$$

where ρ is the mass density of the particle and g is the gravitational acceleration.

2.1.4 Lifting electric field

For the configuration of a spherical particle on a grounded plane in Figure 2.1, the lifting electric field E_L of this electrode system can be determined from equations (2.4) and (2.5).

$$E_L = \sqrt{\frac{g\rho R}{3\times 1.369\varepsilon_0}} \approx 5.19\times 10^5 \sqrt{\rho R} \tag{2.6}$$

For the gap *d*, the lifting voltage V_L is

$$V_L = E_L d \tag{2.7}$$

The lifting electric field E_L varies linearly with the square root of mass density and radius of the particles. This thesis considers the aluminum, steel and stainless steel sphere, which have mass density about 2700, 7725 and 8006 kg/m^3, respectively. Figure 2.2 shows the lifting electric field E_L as a function of particle radius *R* for the calculation. The graph shows that E_L increases with the particle radius *R*. E_L of the aluminum particle is smaller than that of steel and stainless steel particles according to the densities these materials.

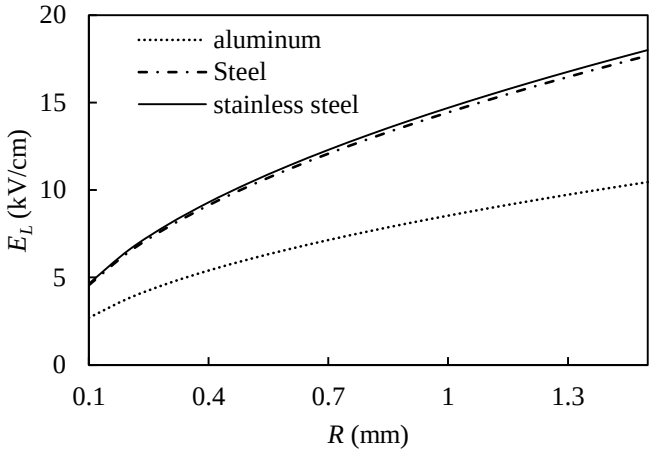

Figure 2. 2. Lifting electric field as a function of particle radius.

2.2 Adhesion between particle and plate electrode

Consider a conducting spherical particle on the conducting plate electrode as shown in Figure 2.3. The contact of particle and plate electrode causes the adhesion force F_{ad} , which includes the Van der Waal F_{vdw} , capillary F_{cap} and surface roughness force F_{roug}. Therefore, the adhesion force can be written as

$$F_{ad} = F_{vdw} + F_{roug} + F_{cap} \tag{2.8}$$

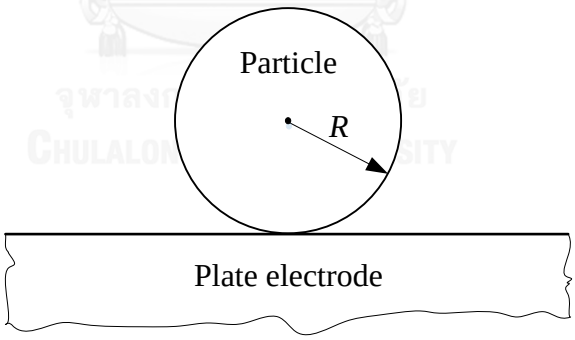

Figure 2. 3. Particle lying on plate electrode.

The Van der Waal force F_{vdw} depends on the particle size and material type of particle and electrode, which is around 85±25 nN for the metals particle of 2 ±0.5 μm radius [16]. The capillary force F_{cap} is from the capillary condensation of water at the contact region, which depends on the humidity. The capillary force has small when the humidity is around 50% and become more prominent at over 70% for the particles of 9

-11 μm diameter [17]. For the surface roughness forces F_{roug}, this thesis considers a smooth spherical particle of radius *R* on the ground electrode with surface roughness as shown in Figure 2.4. The surface roughness forces is increased with increasing particle sizes or reduced with increasing size of asperity. For the size of particle similar or smaller than the asperity (*r*) of plate electrode, the force increases with surface roughness [18].

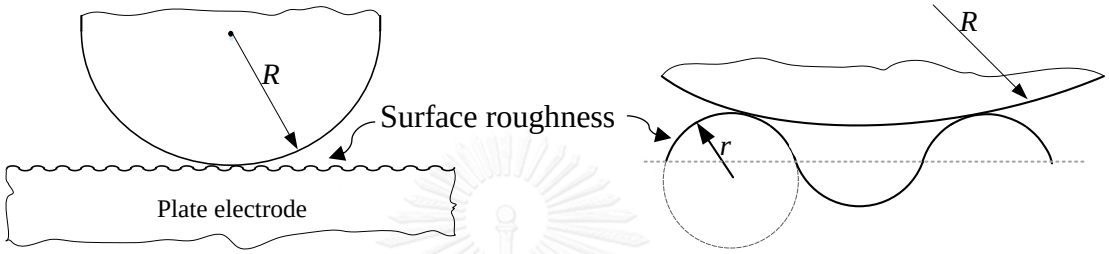

(a) Particle contact with surface roughness (b) Contact point

Figure 2. 4. Smooth particle lying on the surface roughness with ground electrode.

2.3 Gas density

In this thesis, the gas density is varied by using a mixture of air and SF_6 or N_2 in the chamber. The ideal gas law can be used to calculated gas density.

$$pV = nR_gT \tag{2.9}$$

where *p* is pressure (bar), *V* is volume (m^3). *n* is number of moles, R_g is universal gas constant (0.0821 L.atm/mol.K) and *T* is temperature (K).

The density *D* is the mass *m* of the gas per unit volume.

$$D = \frac{m}{V} = \frac{nM}{V} \tag{2.10}$$

where *M* is molar mass.

This thesis uses a mixture of air and SF_6 (air/SF_6 mixture) or N_2 (air/N_2 mixture) with a molar proportion to 1:1. The molar mass of air, N_2 and SF_6 is 28.964, 28.013 and 146.06 g/mol, respectively. Therefore, the density of air/SF_6 mixture for 1 bar gas pressure is approximate to the air and air/N_2 mixture at 3 bar pressure as shown in Table 2.1.

Table 2. 1. Density of air and gas mixture at 30ºC

P (bar)	Density (kg/m^3)		
	air	air/N_2	air/SF_6
1	1.160	1.144	3.515
3	3.462	3.403	10.455

CHAPTER 3
EXPERIMENTS

3.1 Experimental setup

The schematic diagram of the experimental setup is shown in Figure 3.1. The main components were a DC high voltage source, a measurement equipment, a chamber and an electrode system. The DC high voltage was generated from 220V 50 Hz AC voltage by using a test transformer (220 V/100 kV, 5 kVA) and a two-step full-wave rectifier circuit. The voltage was applied to the electrode system through a 13.9 MΩ current limiting resister. For experiments under gas pressure, the electrodes were installed in a chamber, as shown in Figure 3.2. The pressure in the chamber was set to 1, 2 or 3 bar. A resistive voltage divider and a multi voltage meter (FLUKE 278 TRUE RMS) were used to measure the applied voltage. Calibration was carried out for the divider on the range of voltage used in the experiments.

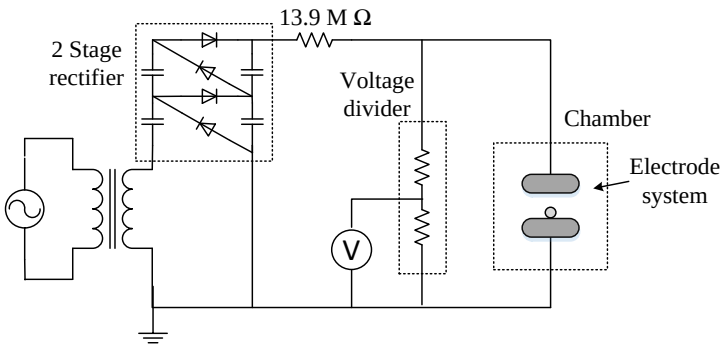

(a) Circuit diagrams

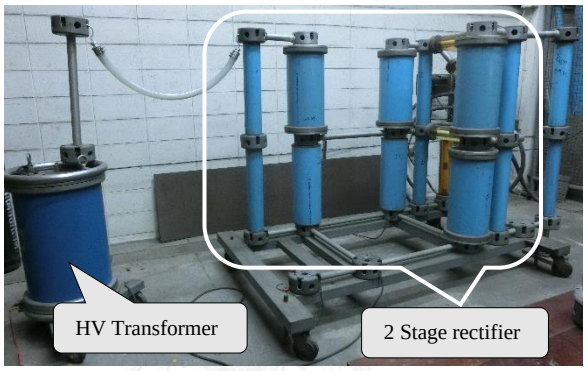

(b) Images of DC high voltage source

Figure 3. 1. Experimental setup.

3.1.1 Chamber

All experiments were done in a test chamber. Figure 3.2(a) shows the schematic diagram of the test chamber used for experiments under the different gas pressures. Figures 3.2(b) and 3.2(c) show the image of the test chamber and arrangement inside the chamber. The chamber was made from steel. It can withstand absolute pressure higher than 3 bar, and had two windows at the same height but separated by 90^{o} for illumination and for observation. The lower electrode was placed on the xyz-axis stage, which was set on the floor of the chamber. The upper electrode was attached to the chamber cover. The inlet/outlet of air and the compound gauge (as shown in Figure 3.2(d)) were installed.

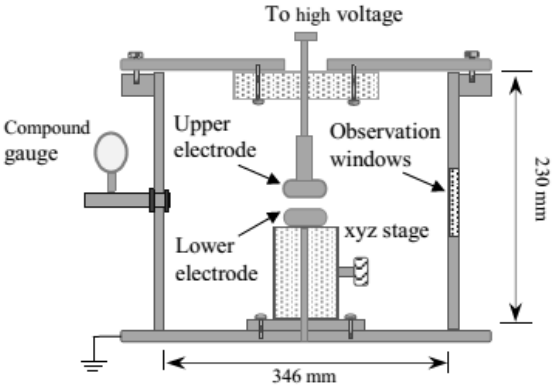

(a) Schematic diagram of test chamber

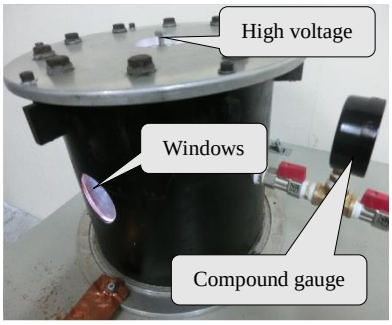

(b) Images of test chamber

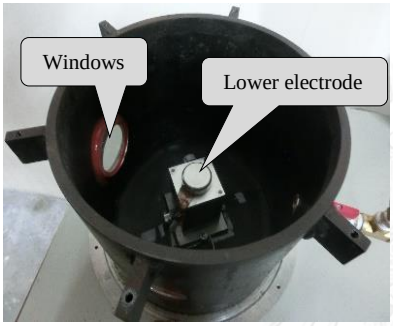

(c) Arrangement inside the chamber

(d) Compound gauge

Figure 3. 2. Test chamber for experiments in pressurized conditions.

3.1.2 Electrode system

The electrode system consisted of two parallel discs made of stainless steel, as shown in Figure 3.3. An aluminum disc of the same dimensions was used as the lower electrode for some cases. The electrodes had 20 mm radius and 15 mm thickness for both material types. Their edges were curved to prevent excessively high electric field. The upper electrode was connected to the applied voltage. The lower electrode one was grounded. The electrode gap was set to 10 mm for all the experiments.

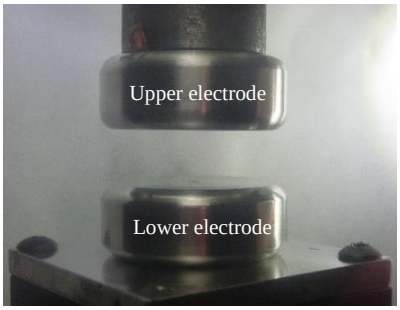

Figure 3. 3. Parallel electrode system.

3.1.3 Particles

The particle samples were made from various materials such as aluminum, stainless steel and steel. The mass density and radius of the particle are summarized in Table 3.1. Three samples were used for each material and size of particle. All particles were cleaned by the acetone and using an ultrasonic cleaner, and then dried by oven with 60^{o}C before use. The smooth surface of the particles is shown in Figure 3.4.

Table 3. 1. Details of the conducting spherical particles.

No	Materials	Radius (mm)	Density (kg/m^3)
1	aluminum	0.4, 0.6, 1.19	2700
2	steel	0.5	7725
3	stainless steel	1	8006

(a) *R*=0.4 mm (aluminum)

(b) *R*=0.68 mm (aluminum)

(c) *R*=1.19 mm (aluminum)

(e) *R*=0.5 mm (steel)

(g) *R*=1 mm (stainless steel)

Figure 3. 4. Images of conducting spherical particles.

3.1.4 Gas medium

According to the experiments with the particle liftoff under pressure, the gas medium was the air and gas mixture of air and SF_6 or N_2. The air was fed into the chamber by using a compressor pump. The humidity of the air varies with experiments. The maximal humidity of air was limited to 60% for all the experiments. The purity of SF_6 and N_2 was 99.9 and 99.995%, respectively. The molar proportion of gas mixtures is 1:1. Therefore, the absolute humidity of gas mixture is reduced by 50% than that of air.

3.2 Calibration of voltage divider

In order to increase the accuracy of experimental results, the DC voltage divider was calibrated. A high voltage probe (Tektronix P6015A) and Oscilloscope (Tektronix TBS 1022) were used to measure the high voltage side of the divider. A multimeter (FLUKE 287 TRUE RMS) measure the low voltage, as shown in Figure 3.5. The applied voltage was increased by step voltage about 1 kV, from 1 kV to 20kV at high voltage side. The calibration was done at 65% RH and 31ºC. As the divider ratios are

practically independent of polarity, the calibration curve (from polarity voltage) in Figure 3.6 is used.

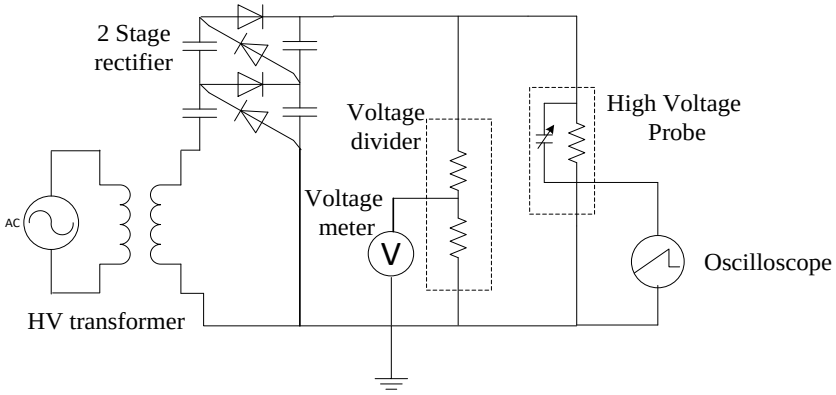

Figure 3. 5. Calibration setup of DC voltage divider.

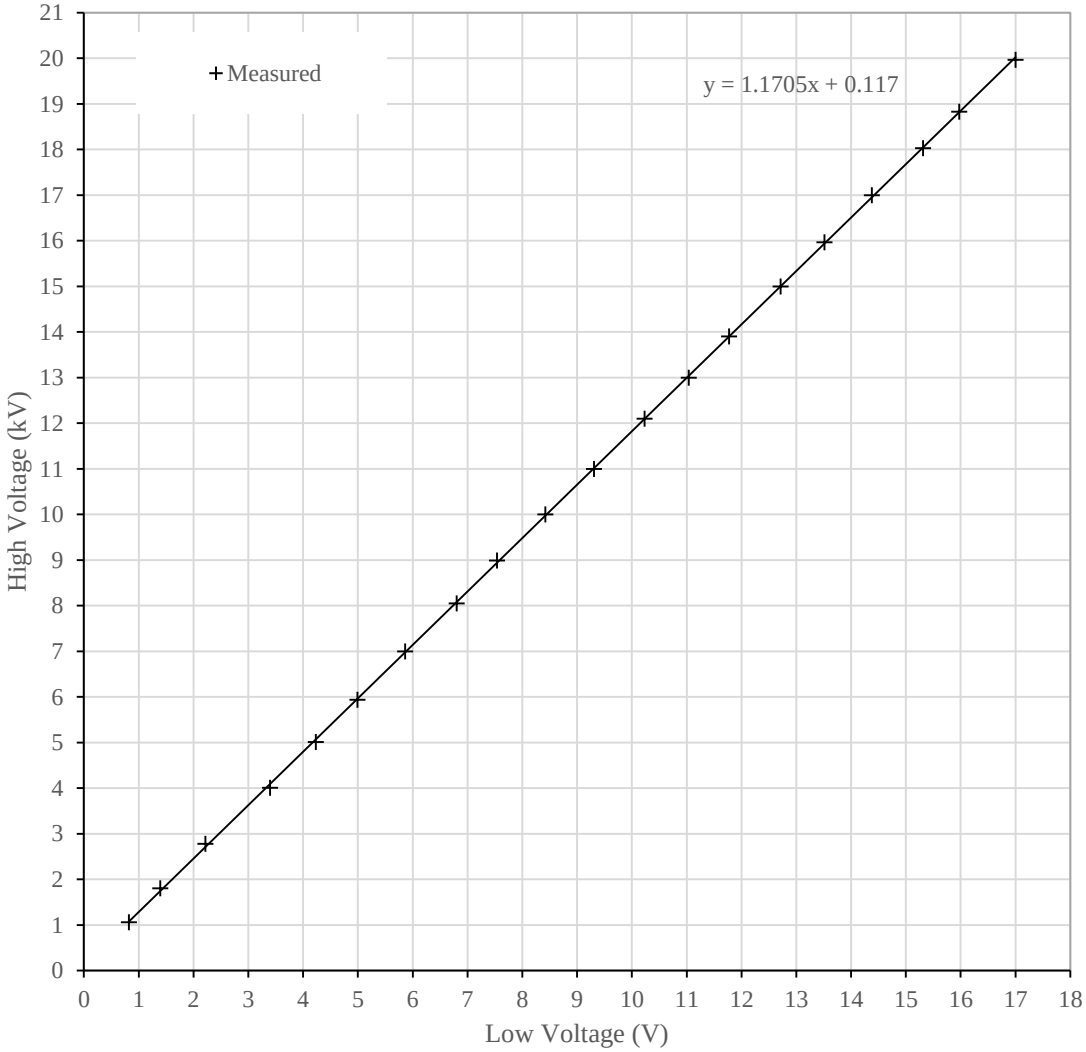

Figure 3. 6. Relation between high voltage and low voltage of DC voltage divider.

3.3 Experimental procedure and condition

In the experiments, a particle was placed on lower (ground) electrode. A DC positive or negative voltage was applied to the upper electrode. The applied voltage was increased gradually with a step of about 0.06 kV until the particle lifted from lower electrode. The experiments were repeated 10 times on each particle for an applied voltage polarity (That is, 30 times for a combination of particle size, gas pressure and voltage polarity). All experimental conditions of this thesis are listed in Table 3.2.

Table 3. 2. Experimental conditions of each particle.

Gas	Materials		Radius of particles (mm)	Pressures (bar)				
	Ground electrode	Particle		0.55	0.75	1	2	3
air	stainless steel	aluminum	0.4	×	×	○	○	○
			0.68	○	○	○	○	○
			1.19	○	○	○	○	○
air/SF_6	stainless steel	aluminum	0.4	×	×	○	×	○
			0.68	×	×	○	×	○
			1.19	×	×	○	×	○
air/N_2	stainless steel	aluminum	0.4	×	×	○	×	○
			0.68	×	×	○	×	○
			1.19	×	×	○	×	○
air	stainless steel	stainless steel	1	×	×	○	○	○
	aluminum	aluminum	0.4	×	×	○	×	○
	aluminum	steel	0.5	×	×	○	○	○

○: Tested

×: Untested

CHAPTER 4
RESULTS AND DISCUSSION

4.1 Liftoff under different gas pressures

4.1.1 In air

Experiments on the particle liftoff in the air were done with aluminum, stainless steel and steel spheres. The upper and lower electrodes were stainless steel, as shown in Table 3.2. The experimental results are explained as follows.

4.1.1.1 Aluminum particle

For aluminum particle liftoff in the air, the pressure of air is varied between 0.55 to 3 bar. Three sizes (R=0.4, 0.68 and 1.19 mm) of aluminum particles are used. Figure 4.1 shows the cumulative distribution of particle liftoff. The distribution includes results from both polarities. The effect of gas pressure can be seen from the figures. The lifting electric field E_L increases with increasing pressures p for each particle size. However, the variation of the minimal E_L is smaller than that of the maximal E_L for 0.4 mm particle in Figure 4.1(a) and for the 0.68 mm particle under 2 and 3 bar pressure in Figure 4.1(b). On the other hand, both minimal and maximal E_L increase with p approximately by the same extent for the 1.19 mm particle in Figure 4.1(c). In addition, the lifting electric field E_L in Figure 4.1 is increased with particle radius R for each pressure.

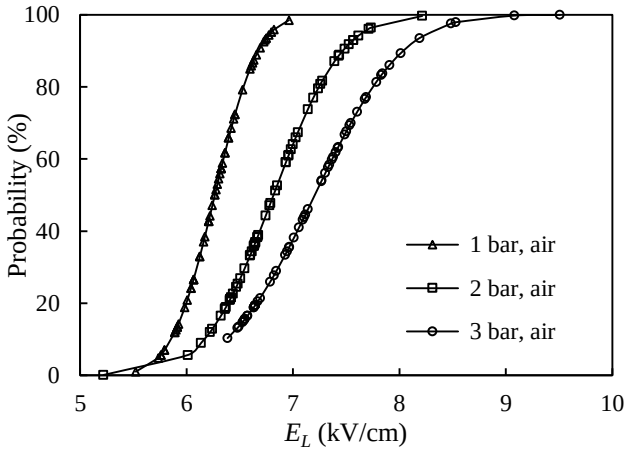

(a) R = 0.4 mm

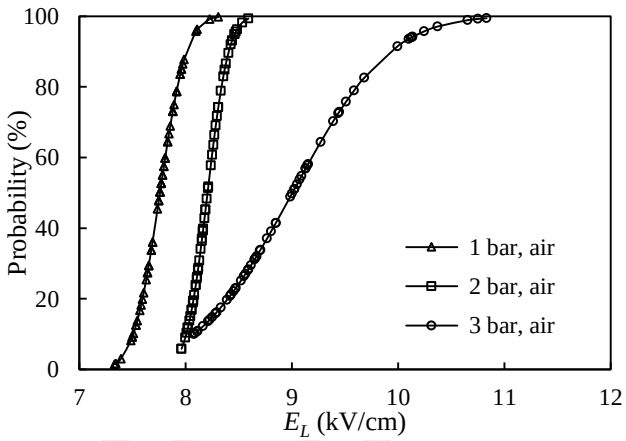

(b) R = 0.68 mm

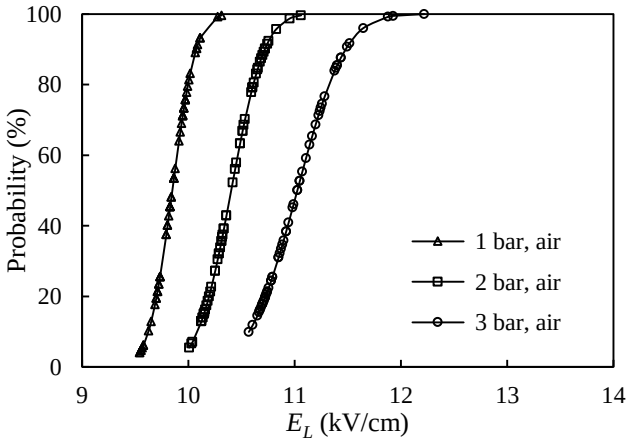

(c) R = 1.19 mm

Figure 4. 1. Cumulative distribution of liftoff of aluminum particles as a function of electric field.

4.1.1.2 Steel and Stainless steel particles

For steel and stainless steel particle liftoff in the air, the pressure of air is varied from 1 to 3 bar. The radius of steel particle was 0.5 mm and stainless steel was 1 mm. Figure 4.2 shows the cumulative distribution of particle liftoff as function of electric field. It can be clear that the effect of gas pressure has the same tendency as the case of aluminum particles. The lifting electric field E_L is increased with the pressures for each particle size.

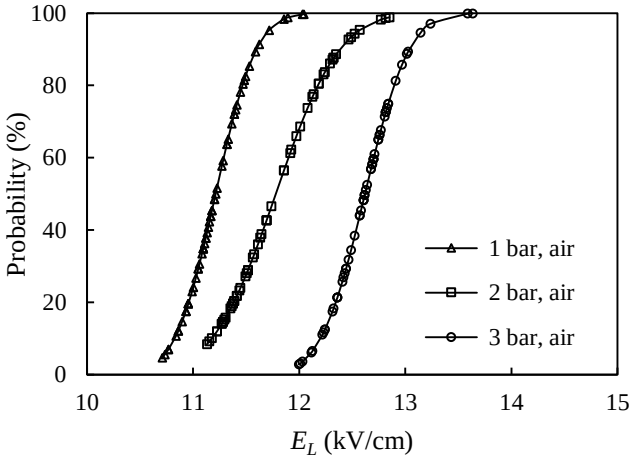

(a) R= 0.5 mm (steel)

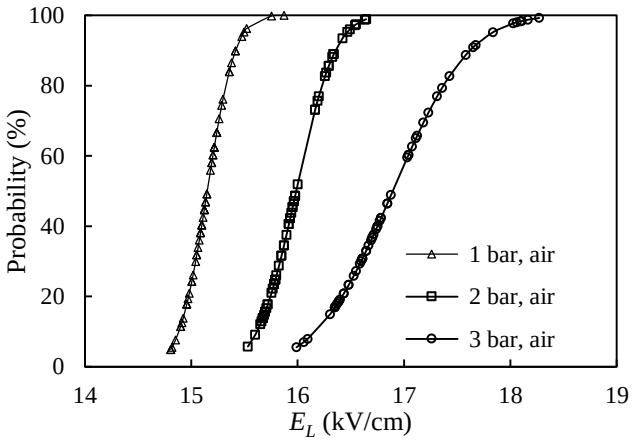

(b) R=1 mm (stainless steel)

Figure 4. 2. Cumulative distribution of liftoff of steel and stainless steel particles as function of electric field.

4.1.1.3 Force difference

Figure 4.3 shows the variation of ΔF with πpR^2 of all particle sizes and pressure values for particle liftoff in the air. ΔF is the difference between the electrostatic force F_e and particle weigh *W*, which can be calculated by

$$\Delta F = F_e - W \tag{4.1}$$

Overall, ΔF increases with the πpR^2 approximately by a linear relationship for all sizes and materials of particle, as shown in Figure 4.3. This implies that the contribution from pressure *p* on the surface force varies with the contact area, which depends on the particle surface area.

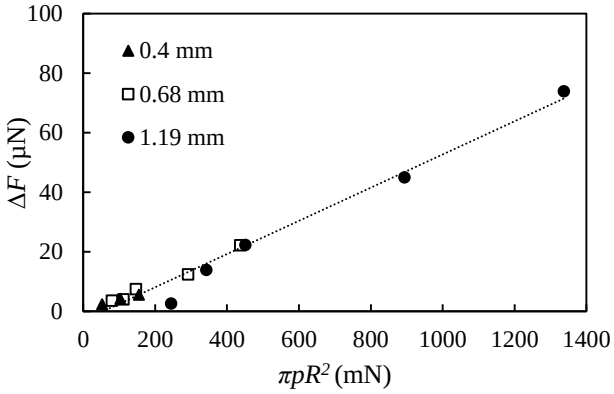

(a) aluminum particle

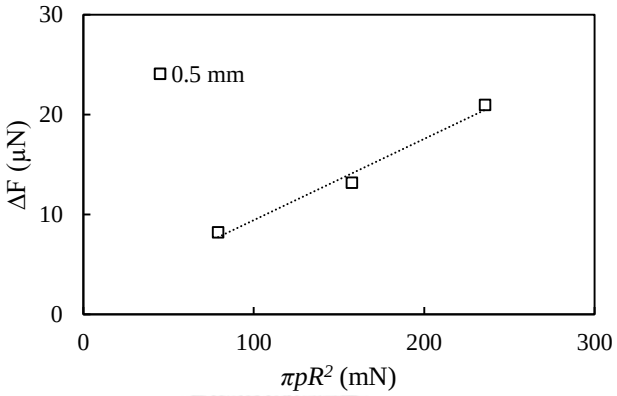

(b) steel particle

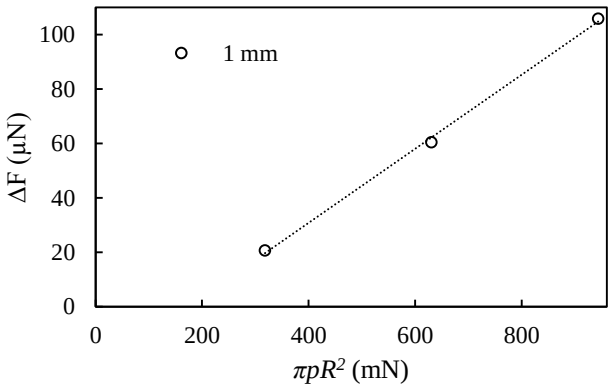

(c) stainless steel particle

Figure 4. 3. Variation of ΔF with πpR^2 of particles and pressures for in the air.

4.1.2 Different gas media

We carried out experiments on the liftoff of aluminum particle in the mixture of air and SF_6 (air/SF_6), and air and N_2 (air/N_2). The pressure was 1 and 3 bar. The three sizes (R=0.4, 0.68 and 1.19 mm) of the aluminum particles were used. The proportion of gas mixture was 1:1, as explained in section 3.1.4.

Figure 4.4 shows the cumulative distribution of particle liftoff in the air/SF_6 mixture and air/N_2 mixture as a function of E_L in comparison with the results in the air. It is clear that the effect of gas pressure has the same tendency as that in the air. That is, E_L increases with the pressures for both gas media. The comparison shows that E_L in the air/SF_6 mixture is smaller than that in the air for all conditions. The difference between E_L in the air and air/SF_6 media is smaller under 1 bar pressure than under 3 bar for each particle size. In addition, the particle liftoff in the air/N_2 mixture shows the same electric field values with that in the air for the cases of 0.4 and 0.68 mm particle radius under 1 bar pressure as shown in Figures 4.4(a) and 4.4(b). On the other hand, the 3 bar pressure shows that the lifting electric field E_L in the air/N_2 mixture has the same values to the air/SF_6 mixture. Also the liftoff of big particle (R=1.19 mm) in Figure 4.4(c), E_L in the air/N_2 mixture exhibits the same value to the air/SF_6 mixture and is smaller than that in the air for each pressure. Most of the cases in Figure 4.4 show that E_L in the gas mixture is smaller than that in the air. The different E_L between air and gas mixtures is caused by the effect of humidity because the humidity of the gas mixture is smaller than of the air as explained in section 3.1.4. The humidity makes the capillary condensation of water at surface contact between particle and grounded electrode. The capillary force increases the particle adhesion to the grounded electrode.

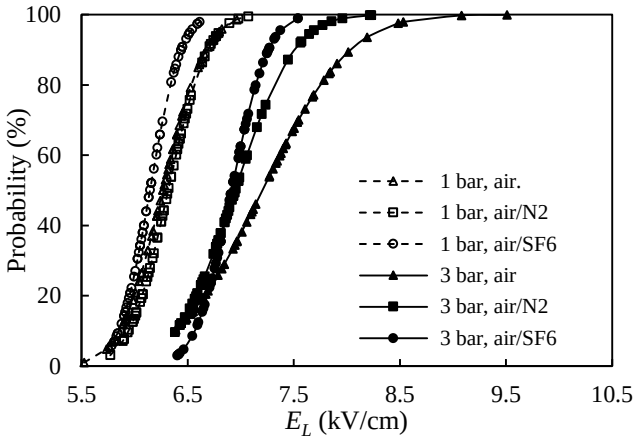

(a) R = 0.4 mm

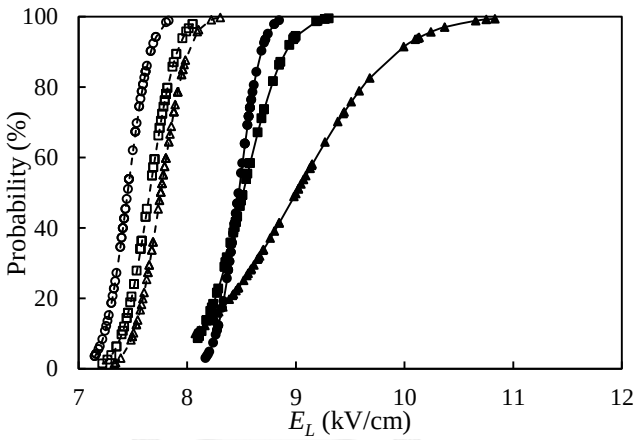

(b) R = 0.68 mm

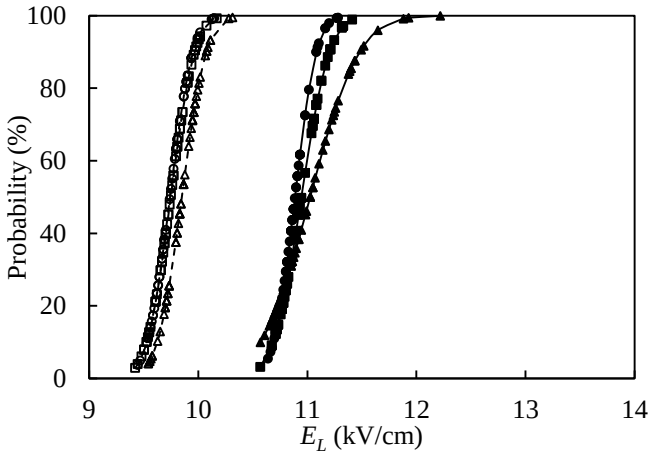

(c) R = 1.19 mm

Figure 4. 4. Comparison of the cumulative distribution of liftoff for aluminum particles in the air, air/SF_6 and air/N_2 media.

4.1.3. Discussion

The lifting electric field in the air/SF_6 and the air/N_2 mixture was comparable to each other in the Section 4.1.3. This section considers the particle liftoff in the air and in the air/SF_6 mixture. The average lifting electric field of the aluminum particle liftoff is shown in Figure 4.5. The average values are taken from the results of both polarities. The analytical liftoff electric field is also given in the figure for comparison. The measurement results in the figure show the same tendency as analytical E_L. All measured values are higher than the analytical one. This indicates the effect of the adhesion force between particle and ground electrode. The total adhesion force is the summation of van der Waals, capillary and surface roughness forces. They depend on the contact condition and play a role on the particle liftoff.

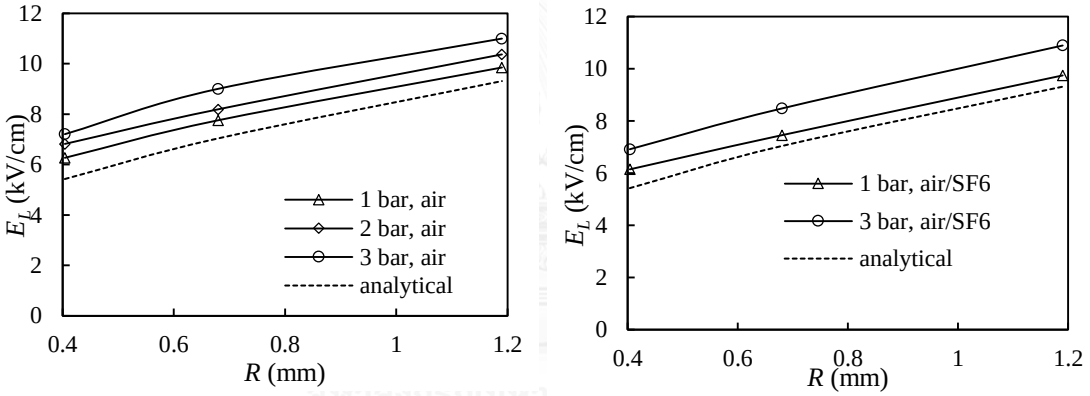

(a) in air (b) in air/SF_6 mixture

Figure 4. 5. Average lifting electric field E_L as a function of particle radius R.

The difference between E_L from the experiments in comparison with the analytical one is presented in Figure 4.6. Note that

$$\Delta E_L(\%) = \frac{E_{L,EXP} - E_{L,ANA}}{E_{L,ANA}} \times 100 \tag{4.2}$$

where the subscripts *EXP* and *ANA* denote the field from the experiments and analysis, respectively.

It can be seen from Figure 4.6 that ΔE_L decreases nonlinearly with particle radius R. The effect of R on E_L reduces with increasing the particle sizes.

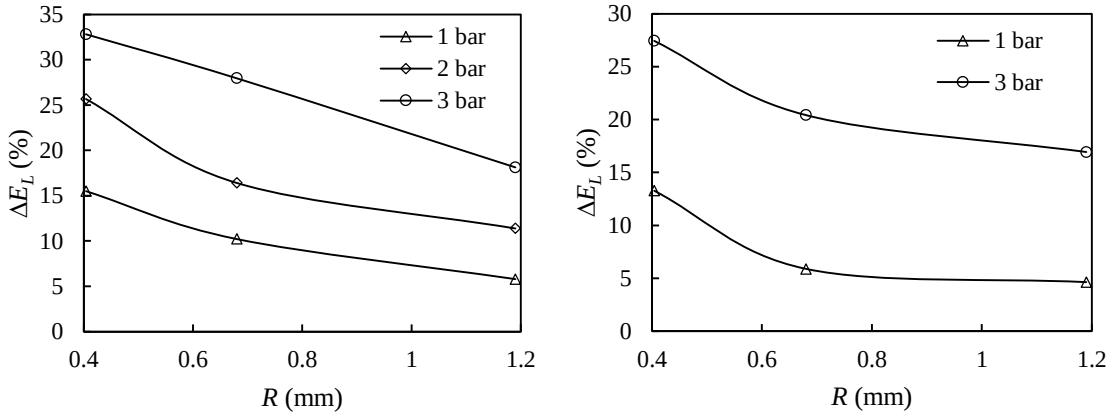

(a) in air (b) in air/SF_6

Figure 4. 6. ΔE_L as function of R.

Figure 4.7 shows the force difference ΔF as function of πpR^2 for aluminum particle liftoff in the air and in the air/SF_6 mixture. ΔF for the particle liftoff in the air is explained in section 4.1.1.3. We can be seen from this figure that ΔF for the particle liftoff in the air/SF_6 mixture is the same tendency as that in the air. ΔF also increases with πpR^2 approximately by a linear relationship. However, ΔF of particle liftoff in the air/SF_6 mixture exhibits smaller than that in the air.

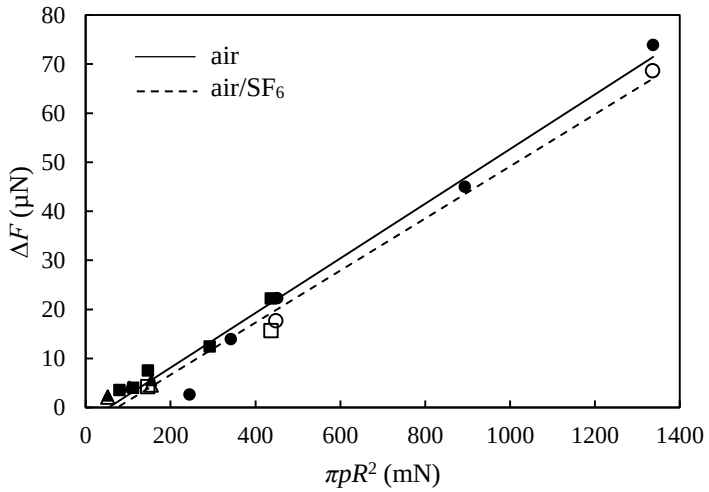

Figure 4. 7. Variation of ΔF with πpR^2 of particles and pressures. The symbols Δ, □ and ○ denote the cases of 0.4, 0.68 and 1.19 mm radius, respectively.

4.2 Voltage polarity

The experiments are carried out by applying DC positive and negative voltage to the upper electrode. The particle on the grounded electrode is negatively charged by

positive voltage application and vice versa. In this section, we consider the effects of applied voltage polarities on particle liftoff in the air and gas mixtures. The aluminum grounded electrode is used for some experiments.

4.2.1 In air

The cumulative distribution of particle liftoff as a function of electric field is shown for each voltage polarity in Figure 4.8. The solid and dashed lines are the positive and negative voltage application, respectively. Figures 4.8(a) and 4.8(b) show that the effect of voltage polarity is small for the particle radius of 0.68 and 1.19 mm under 1 or 2 bar pressure although the particles tended to lift at slightly higher electric field for the positive voltage. On the other hand, the smallest particle (R = 0.4 mm) exhibits noticeable dependency of the liftoff on the voltage polarity under all pressure values. In particular, the cases of 3 bar pressure shown that the effect of the applied voltage becomes more clearly in Figure 4.8(c) for all particle sizes. It can be also seen from Figure 4.8 that for most cases where the polarity effect is noticeable, the particles exhibits larger difference in the maximal lifting field than in the minimal field.

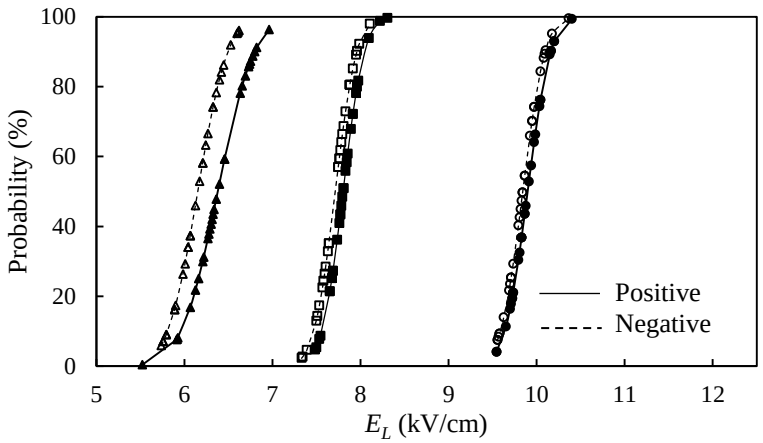

(a) 1 bar

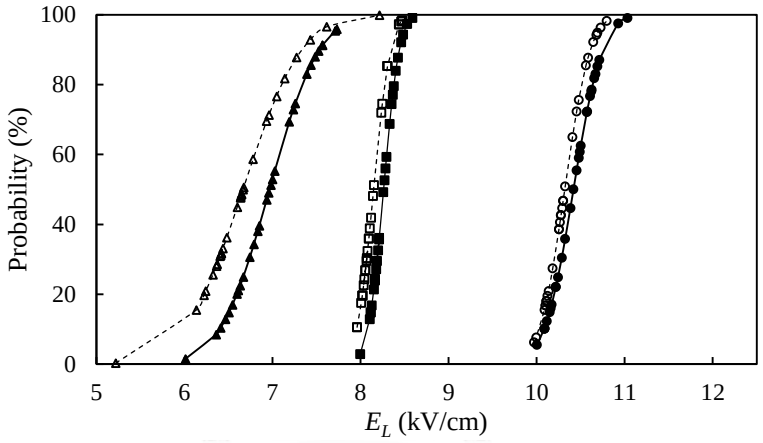

(b) 2 bar

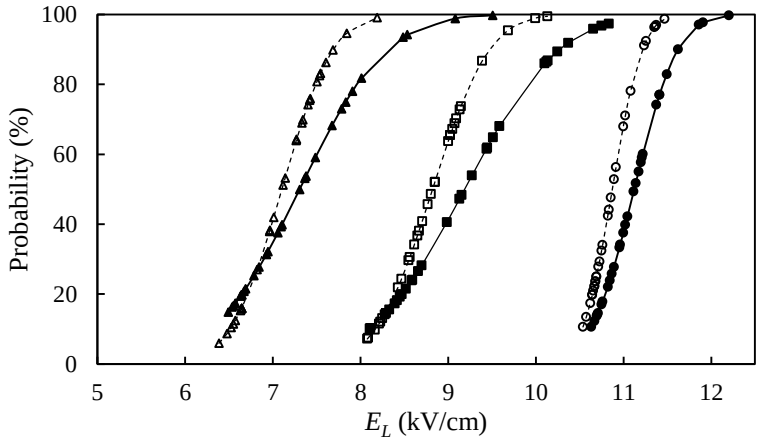

(c) 3 bar

Figure 4. 8. Cumulative distribution of particle liftoff in the air for each applied voltage polarity. The symbols Δ, □ and ○ denote the cases of 0.4, 0.68 and 1.19 mm radius, respectively.

Figure 4.9 summarizes the average values of the lifting electric field E_L for cases of 3 bar pressure. The standard deviation of the measured data is also given on the graph. The graph illustrates the average values of the lifting electric field E_L for comparison between positive and negative polarity. We can see small but consistent effect of voltage polarity for all the particle sizes. Even though the distributions in Figure 4.9 are quite different between the polarities. The average E_L differs around 2.85, 4.14 and 2.29% for the cases of 0.4, 0.68 and 1.19 mm radius, respectively. On the other hand the maximal E_L in Figure. 4.8(c) differs around 16, 6.91 and 6.37% for the corresponding cases.

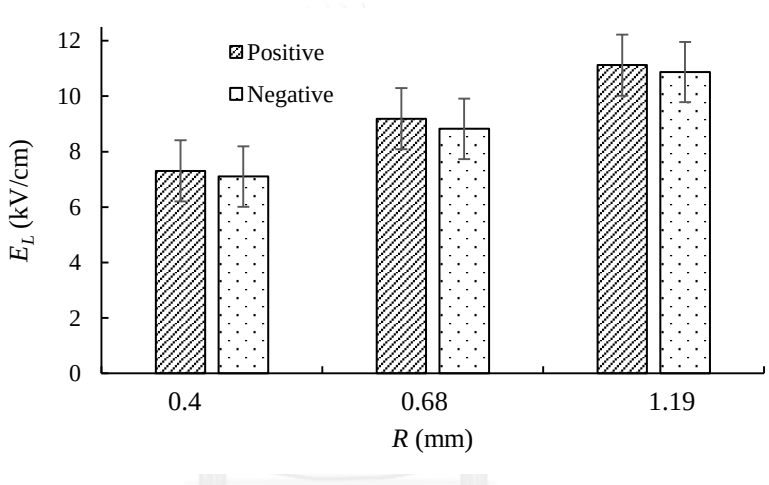

Figure 4. 9. Average E_L in the air under 3 bar pressure for aluminum particle and stainless steel electrode.

4.2.2 In gas mixtures

This section explains the particle liftoff under 1 and 3 bar pressure in the air/SF_6 mixture, and air/N_2 mixture. The cumulative distribution of particle liftoff as a function of electric field for each voltage polarity is shown in Figures 4.10 and 4.11 for cases of air/SF_6 and air/N_2, respectively. We can see from the figure that the liftoff of particles still have the effect of voltage polarity. The lifting electric field for positive voltage application is slightly higher than negative polarity. The tendency observed for all particle sizes, pressures and gas media. However, the effect of voltage polaity is significantly reduced for gas mixtures.

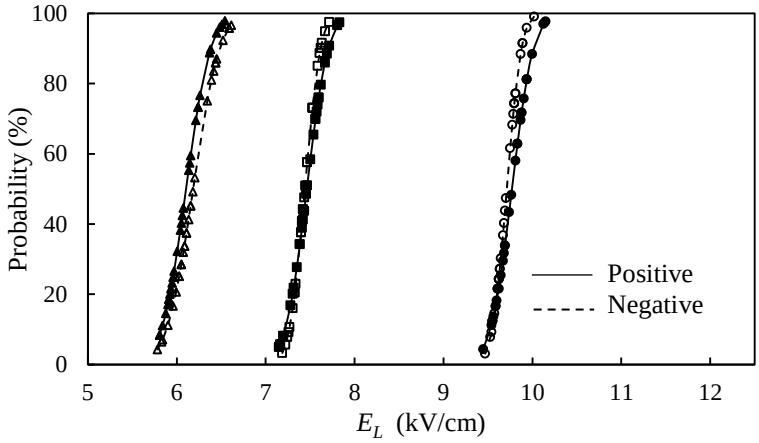

(a) p = 1 bar

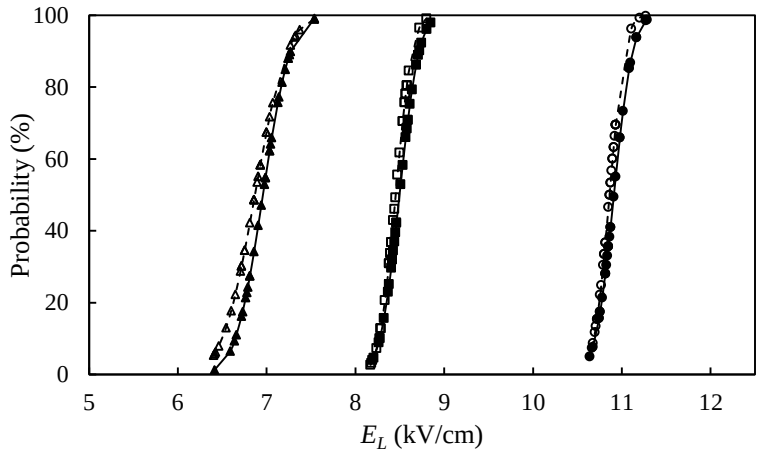

(b) p = 3 bar

Figure 4. 10. Cumulative distribution of particle liftoff in the air/SF_6 mixture for each voltage polarity as a function of electric field. The symbols Δ, □ and ○ are the same as those in Figure 4.8.

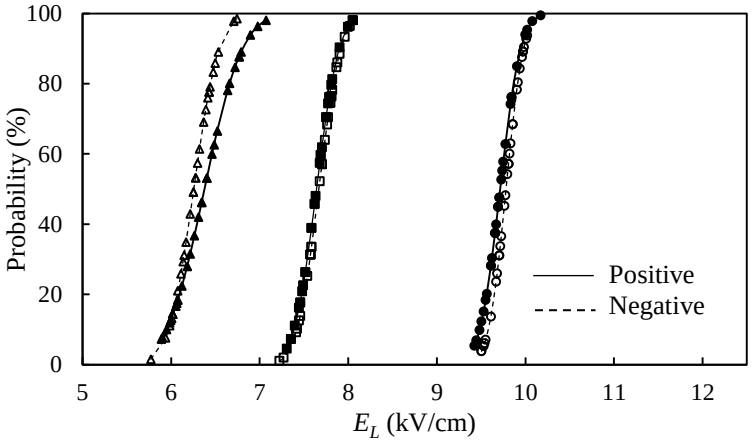

(a) p = 1 bar

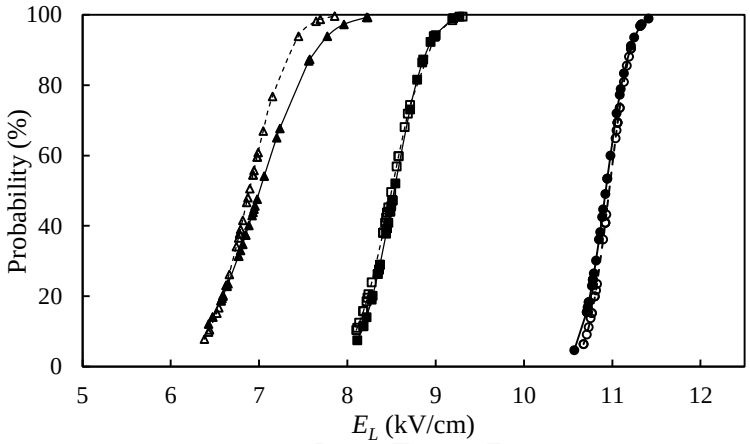

(b) p = 3 bar

Figure 4. 11. Cumulative distribution of particle liftoff in the air/N_2 mixture for each voltage polarity as a function of electric field. The symbols Δ, □ and ○ are the same as those in Figure 4.8.

4.2.3 Different materials

The effect of voltage polarity on the particle liftoff may be caused by material types of particle and electrode which have different work functions. To clarify the different lifting electric field between polarities of the particle in the experiments, the variation of material types for the particle and ground electrode are used. The materials of particle and electrode are shown in Table 4.1.

Table 4. 1. Materials of particles and grounded electrode.

Electrode	Particle	Radius of particle (mm)
aluminum	aluminum	0.4
stainless steel	stainless steel	1
aluminum	steel	0.5

The cumulative distribution of particle liftoff as a function of electric field when the particle and electrode are of the same material is shown in Figure 4.12. As is illustrated by the graph, the effect of voltage polarity is very small for the aluminum particle and electrode in Figure 4.12(a). For the stainless steel particle and grounded electrode in Figure 4.12(b), the particles tended to lift at the similar electric field values of both voltage polarities for 1 bar pressure. The liftoff under 3 bar pressure exhibits the small dependency on the voltage polarity.

For the case in which the particle and electrode materials are reversed from those in previous sections in Figure 4.12, the lifting electric field of positive voltage is smaller than negative polarity for each pressure. Therefore, the aforementioned results indicate strong dependency of the polarity effect on the materials involved.

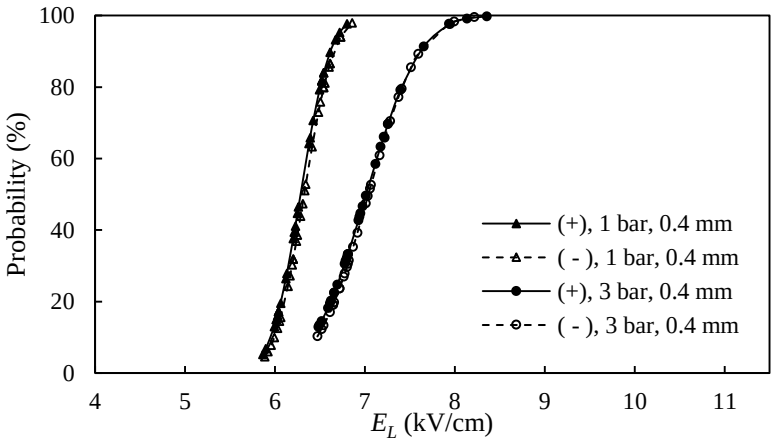

(a) aluminum particle and ground electrode

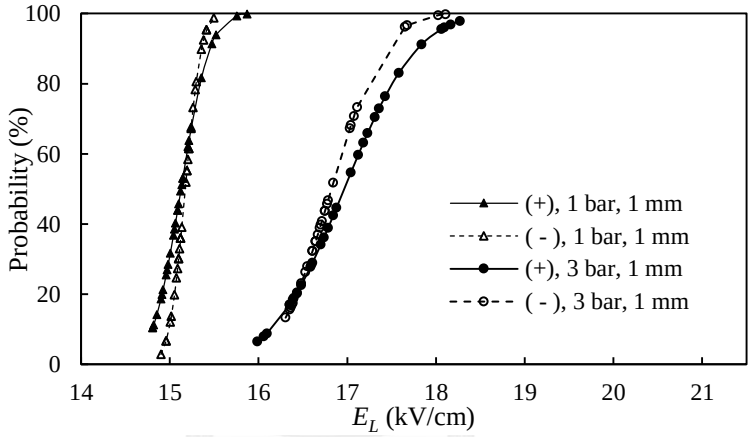

(b) stainless steel particle and ground electrode

Figure 4. 12. Cumulative distribution of particle liftoff as a function of electric field for the similar particle and electrode material.

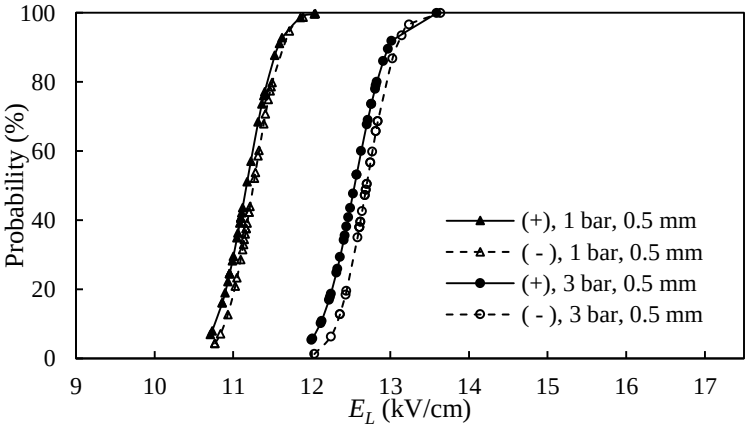

Figure 4. 13. Cumulative distribution of particle liftoff as a function of electric field for the steel particle and aluminum grounded electrode.

CHAPTER 5
CONCLUSIONS

This work studies experimentally the liftoff of conducting spherical particles in a uniform electric field under different gas media and pressures. The pressure of air, air/SF_6 mixture and air/N_2 mixture is used, where the proportional of gas mixture is 1:1. The conducting spherical particles are aluminum, stainless steel and steel spheres. The particle sizes and varied pressures are explained in Table 3.2. The effects of gas pressure are clearly observed from our results, which can be summarized as follows.

For the particle liftoff in the air, the lifting electric field increases significantly with increasing gas pressures for each material and size of particle. The difference between electrostatic force and particle weigh increases with $\pi p R^2$ approximately by a linearly relationship for aluminum, stainless steel and steel particles. This is the contribution from pressure on the surface force varies with the contact area, which depends on the particle surface area.

For the particle liftoff in the different gas medium, the lifting electric field also increases with increasing pressures and particle sizes for all gas medium. The lifting electric field in the air/SF_6 mixture and air/N_2 mixture is smaller than that in the air due to the reduced capillary force at surface contact between particle and grounded electrode. The difference between lifting electric field in the air and gas mixture is smaller under 1 bar pressure than 3 bar for each particle size. The difference between electrostatic force and particle weigh also increases with $\pi p R^2$ approximately by a linearly relationship for all gas media. The force difference of gas mixtures is smaller than the air for all particle sizes and pressures.

In addition, the average lifting electric field of measurement results are higher than the analytical values for all gas media. That is caused by the effect of the adhesion force, which depends on the contact condition. The difference between lifting electric field from the experiments and analytical is decreased nonlinearly with particle radius.

For the voltage polarity, the effects of voltage polarity are clearly observed in the air under 3 bar pressure for all particle sizes, where the lifting electric field of positive voltage is higher than that of negative voltage application. Under 1 or 2 bar

pressure, only the cases of 0.4 mm particle radius shows the obvious effect of voltage polarity but not significantly reduced in the cases of 0.68 and 1.19 mm particle radius. In the air/SF_6 mixture and air/N_2 mixture, the particle liftoff shows the small effects of voltage polarity for all particle sizes and gas pressures. The lifting electric field for positive voltage application slightly higher than negative polarity.

REFERENCES

[1] R. Nagarsheth and S. Singh, "Study of gas insulated substation and its comparison with air insulated substation," *International Journal of Electrical Power & Energy Systems,* vol. 55, pp. 481-485, 2// 2014.

[2] H. Meinecke, "High voltage gas insulated switchgear: an overview," in *GIS (Gas-Insulated Switchgear) at Transmission and Distribution Voltages, IEE Colloquium on (Digest No.1995/203),* 1995, pp. 3/1-3/8.

[3] N. Phansiri, "Stuldy on the movement of conducting particles under non uniform electric field " Master's Thesis, Department of electrical engineering, Faculty of Engineering, Chulalongkorn University, 2012.

[4] S. Sangkasa-ad, *High Voltage Engineering*, 3 ed. Impression, Bangkok, 2549.

[5] A. H. Cookson, O. Farish, and G. M. L. Sommerman, "Effect of Conducting Particles on AC Corona and Breakdown in Compressed SF6," *IEEE Transactions on Power Apparatus and Systems,* vol. PAS-91, pp. 1329-1338, 1972.

[6] B. Qi, C. R. Li, Z. Hao, B. B. Geng, D. G. Xu, S. Y. Liu, *et al.*, "Surface discharge initiated by immobilized metallic particles attached to gas insulated substation insulators: process and features," *IEEE Transactions on Dielectrics and Electrical Insulation,* vol. 18, pp. 792-800, 2011.

[7] V. Q. Huynh, "Study on the electromechanics of non-spherical particles under electric field in dielectric system," Doctor's Thesis, Department of Electrical Engineering, Faculty of Engineering, Chulalongkorn University, 2013.

[8] K. I. Sakai, D. L. Abella, Y. Khan, J. Suehiro, and M. Hara, "Experimental studies of free conducting wire particle behavior between nonparallel plane electrodes with AC voltages in air," *IEEE Transactions on Dielectrics and Electrical Insulation,* vol. 10, pp. 418-424, 2003.

[9] J. R. Laghari and A. H. Qureshi, "A Review of Particle-Contaminated Gas Breakdown," *IEEE Transactions on Electrical Insulation,* vol. EI-16, pp. 388-398, 1981.

[10] K. Sakai, S. Tsuru, D. L. Abella, and M. Hara, "Conducting particle motion and particle-initiated breakdown in dc electric field between diverging conducting plates in atmospheric air," *IEEE Transactions on Dielectrics and Electrical Insulation,* vol. 6, pp. 122-130, 1999.

[11] K. I. Sakai, D. L. Abella, Y. Khan, J. Suehiro, and M. Hara, "Theoretical and experimental studies for spherical free-conducting particle behavior between nonparallel plane electrodes with AC voltages in air," *IEEE Transactions on Dielectrics and Electrical Insulation,* vol. 10, pp. 404-417, 2003.

[12] K. Sakai, D. L. Abella, J. Suehiro, and M. Hara, "Lateral motion of wire particles toward decreasing electrode gap regions in atmospheric air," in

Properties and Applications of Dielectric Materials, 2000. Proceedings of the 6th International Conference on, 2000, pp. 817-820 vol.2.

[13] K. Sakai, D. L. Abella, J. Suehiro, and M. Hara, "Charging and behavior of a spherically conducting particle on a dielectrically coated electrode in the presence of electrical gradient force in atmospheric air," *IEEE Transactions on Dielectrics and Electrical Insulation*, vol. 9, pp. 577-588, 2002.

[14] N. Phansiri and B. Techaumnat, "Study on the electromechanics of a conducting particle under nonuniform electric field," *IEEE Transactions on Dielectrics and Electrical Insulation,* vol. 20, pp. 488-495, 2013.

[15] H. Parekh, K. D. Srivastava, and R. G. v. Heeswijk, "Lifting Field of Free Conducting Particles in Compressed SF6 with Dielectric Coated Electrodes," *IEEE Transactions on Power Apparatus and Systems*, vol. PAS-98, pp. 748-758, 1979.

[16] F. L. Leite, C. C. Bueno, A. L. Da Róz, E. C. Ziemath, and O. N. Oliveira, "Theoretical Models for Surface Forces and Adhesion and Their Measurement Using Atomic Force Microscopy," *International Journal of Molecular Sciences,* vol. 13, p. 12773, 2012.

[17] M. Takeuchi, "Adhesion forces of charged particles," *Chemical Engineering Science,* vol. 61, pp. 2279-2289, 4// 2006.

[18] A. Kumar, T. Staedler, and X. Jiang, "Role of relative size of asperities and adhering particles on the adhesion force," *Journal of Colloid and Interface Science,* vol. 409, pp. 211-218, 11/1/ 2013.

APPENDIX

APPENDIX A: The raw data of experimental results for particle liftoff in the air.

Table A 1. The aluminum particle of 0.4 mm radius liftoff under 1, 2 and 3 bar pressure for the stainless steel ground electrode.

(a) p =1 bar

No	E_L of positive (kV/cm)			E_L of negative (kV/cm)		
	Particle 1	Particle 2	Particle 3	Particle 1	Particle 2	Particle 3
1	6.16	6.27	6.66	6.36	5.79	6.60
2	6.22	6.77	6.07	6.21	6.32	5.90
3	6.96	6.40	6.75	6.62	5.73	5.89
4	6.12	6.31	6.74	6.42	6.04	6.21
5	6.63	6.29	5.91	5.98	6.61	6.27
6	5.91	6.82	5.92	6.07	5.76	5.89
7	6.69	6.73	6.45	6.24	6.12	6.01
8	6.80	6.32	6.34	6.07	6.44	5.76
9	6.45	6.21	6.30	6.53	6.32	5.79
10	6.36	5.52	6.28	6.17	6.40	6.04
Average	6.43	6.36	6.34	6.27	6.15	6.03

(b) p =2 bar

No	E_L of positive (kV/cm)			E_L of negative (kV/cm)		
	Particle 1	Particle 2	Particle 3	Particle 1	Particle 2	Particle 3
1	7.39	6.01	7.71	6.24	7.62	6.65
2	7.26	7.57	6.60	6.44	6.67	6.37
3	6.61	7.44	6.96	6.42	6.41	6.67
4	7.24	7.52	7.49	7.43	6.64	6.48
5	7.00	6.98	6.63	6.14	7.27	6.78
6	6.79	7.03	6.93	8.21	5.22	6.41
7	7.73	7.19	6.36	7.05	6.22	7.14
8	6.41	6.74	6.67	6.60	6.65	6.32
9	6.47	6.55	6.50	6.93	6.96	6.64
10	7.57	6.83	6.85	6.42	6.64	6.36
Average	7.05	6.99	6.87	6.79	6.63	6.58

(c) p =3 bar

No	E_L of positive (kV/cm)			E_L of negative (kV/cm)		
	Particle 1	Particle 2	Particle 3	Particle 1	Particle 2	Particle 3
1	7.91	9.51	7.30	7.69	7.53	6.64
2	7.49	7.38	6.79	7.27	7.12	7.50
3	8.01	7.78	8.53	8.19	6.55	7.60
4	9.08	7.68	6.94	6.63	6.64	7.54
5	6.64	6.57	7.37	7.33	7.27	6.38
6	6.69	7.83	6.93	7.34	7.40	7.14
7	8.48	6.64	7.09	7.01	7.84	6.48
8	7.10	6.84	6.67	7.43	7.42	6.57
9	6.63	6.49	6.64	6.82	6.96	6.97
10	6.55	6.54	7.06	6.64	6.64	6.53
Average	7.46	7.33	7.13	7.24	7.14	6.94

Table A 2. The aluminum particle of 0.68 mm radius liftoff under 0.55, 0.75, 1, 2 and 3 bar pressure for the stainless steel ground electrode.

(a) p = 0.55 bar

No	E_L of positive (kV/cm)			E_L of negative (kV/cm)		
	Particle 1	Particle 2	Particle 3	Particle 1	Particle 2	Particle 3
1	7.67	7.62	7.42	7.44	7.41	7.46
2	7.71	7.42	7.61	7.27	7.37	7.66
3	7.47	7.42	7.06	7.57	7.15	7.19
4	7.56	7.51	7.23	7.47	7.22	7.14
5	7.30	7.13	7.51	7.20	7.37	7.30
6	7.29	7.41	7.61	7.30	7.28	7.57
7	7.16	7.40	7.40	7.70	7.42	7.19
8	7.34	7.20	7.30	7.12	7.18	7.32
9	7.35	7.54	7.25	7.29	7.69	7.15
10	7.75	7.77	7.44	7.46	7.21	7.34
Average	7.46	7.44	7.38	7.38	7.33	7.33

(b) p = 0.75 bar

No	E_L of positive (kV/cm)			E_L of negative (kV/cm)		
	Particle 1	Particle 2	Particle 3	Particle 1	Particle 2	Particle 3
1	7.47	7.62	7.39	7.23	7.44	7.83
2	7.75	7.32	7.46	7.26	7.64	7.22
3	7.46	7.21	7.51	7.61	7.12	7.30
4	8.10	7.50	7.30	7.14	7.50	7.47
5	7.12	7.19	7.60	7.87	7.51	7.07
6	7.10	7.34	7.34	7.32	7.57	7.43
7	7.39	7.61	7.33	7.03	7.69	7.61
8	7.57	7.54	7.49	7.28	7.57	7.25
9	7.43	7.35	7.48	7.43	7.19	7.36
10	7.50	7.34	7.53	7.35	7.37	7.57
Average	7.49	7.40	7.44	7.35	7.46	7.41

(c) p = 1 bar

No	E_L of positive (kV/cm)			E_L of negative (kV/cm)		
	Particle 1	Particle 2	Particle 3	Particle 1	Particle 2	Particle 3
1	7.49	7.96	7.89	8.11	7.77	7.76
2	7.91	7.65	7.77	7.95	7.63	7.57
3	7.53	7.84	8.09	7.59	7.50	7.88
4	7.68	7.85	8.24	7.79	7.88	7.51
5	7.68	7.91	7.74	7.58	7.78	7.98
6	7.54	7.50	7.97	7.64	7.75	7.75
7	7.78	7.65	7.81	7.96	7.83	7.33
8	7.69	8.22	7.81	7.53	7.64	7.91
9	7.83	7.76	7.77	7.76	7.81	7.60
10	7.79	7.69	7.95	7.34	7.88	7.39
Average	7.69	7.80	7.90	7.73	7.75	7.67

(d) p = 2 bar

No	E_L of positive (kV/cm)			E_L of negative (kV/cm)		
	Particle 1	Particle 2	Particle 3	Particle 1	Particle 2	Particle 3
1	8.17	8.14	8.26	8.07	8.02	8.06
2	8.05	8.33	8.08	8.47	8.12	8.09
3	8.13	8.28	8.43	8.11	8.07	8.24
4	8.53	8.04	8.30	8.02	8.44	8.04
5	8.09	8.38	8.18	8.46	8.01	8.15
6	8.06	8.59	8.12	8.04	7.96	8.31
7	8.35	8.12	8.09	8.25	8.09	8.02
8	8.48	8.05	8.46	8.44	8.07	8.08
9	8.37	7.93	8.40	8.31	8.06	8.14
10	8.21	8.27	8.17	8.07	8.31	7.96
Average	8.24	8.21	8.25	8.22	8.11	8.11

(e) p = 3 bar

No	E_L of positive (kV/cm)			E_L of negative (kV/cm)		
	Particle 1	Particle 2	Particle 3	Particle 1	Particle 2	Particle 3
1	10.83	8.98	10.12	9.39	8.80	8.23
2	10.14	8.47	10.75	9.99	9.02	8.08
3	8.70	9.13	8.52	8.55	8.56	8.43
4	10.10	9.44	10.24	9.09	8.70	9.68
5	8.59	8.11	8.29	8.85	8.47	8.25
6	9.27	8.39	9.59	8.21	9.15	8.16
7	8.33	10.66	8.42	9.07	9.13	8.09
8	9.45	9.15	8.28	9.02	9.00	9.05
9	8.66	9.51	8.59	8.67	8.77	8.65
10	8.11	10.37	8.45	10.13	8.61	8.85
Average	9.22	9.22	9.12	9.10	8.82	8.55

Table A 3. The aluminum particle of 1.19 mm radius liftoff under 0.55, 0.75, 1, 2 and 3 bar pressure for the stainless steel ground electrode.

(a) p = 0.55 bar

No	E_L of positive (kV/cm)			E_L of negative (kV/cm)		
	Particle 1	Particle 2	Particle 3	Particle 1	Particle 2	Particle 3
1	9.13	9.36	9.48	9.40	9.31	9.79
2	9.50	9.36	9.28	9.82	9.36	9.47
3	9.27	9.57	9.90	9.32	9.31	9.35
4	9.33	9.28	9.20	9.38	9.45	9.56
5	9.27	9.31	9.27	9.54	9.49	9.32
6	9.28	9.22	9.31	9.24	9.34	9.40
7	9.26	9.13	9.74	9.33	9.24	9.28
8	9.15	9.21	9.14	9.35	9.36	9.34
9	9.32	9.41	9.45	9.54	9.32	9.64
10	9.74	9.33	9.26	9.40	9.21	9.24
Average	9.33	9.32	9.40	9.43	9.34	9.44

(b) p = 0.75 bar

No	E_L of positive (kV/cm)			E_L of negative (kV/cm)		
	Particle 1	Particle 2	Particle 3	Particle 1	Particle 2	Particle 3
1	9.49	9.68	9.72	9.24	9.47	9.34
2	9.74	9.89	9.91	9.48	9.55	9.28
3	10.03	9.70	10.05	9.74	9.88	9.33
4	9.54	9.79	9.74	9.40	9.67	9.66
5	9.56	9.68	9.49	9.53	9.59	9.81
6	9.43	9.55	9.64	9.61	9.70	9.67
7	9.67	9.86	9.70	9.64	9.35	9.22
8	9.61	9.91	10.01	9.34	9.86	9.47
9	9.86	9.96	9.81	9.68	9.61	9.52
10	9.64	9.89	10.10	9.59	9.63	9.54
Average	9.66	9.79	9.82	9.52	9.63	9.48

(c) p = 1 bar

No	E_L of positive (kV/cm)			E_L of negative (kV/cm)		
	Particle 1	Particle 2	Particle 3	Particle 1	Particle 2	Particle 3
1	9.79	9.83	10.07	9.82	10.28	9.73
2	9.97	9.72	9.83	10.01	9.95	9.56
3	9.87	9.54	9.96	9.57	9.84	9.97
4	10.31	9.73	9.65	9.63	9.96	9.70
5	9.91	9.54	9.83	9.81	9.58	10.09
6	9.71	9.95	9.88	10.02	9.87	9.92
7	9.98	9.70	9.87	9.83	9.87	9.84
8	9.81	10.08	9.72	9.79	9.69	9.58
9	9.96	10.11	10.08	9.71	9.56	9.95
10	9.94	9.73	10.11	9.99	9.97	9.71
Average	9.93	9.79	9.90	9.82	9.86	9.81

(d) p = 2 bar

No	E_L of positive (kV/cm)			E_L of negative (kV/cm)		
	Particle 1	Particle 2	Particle 3	Particle 1	Particle 2	Particle 3
1	10.38	10.15	10.42	9.97	10.25	10.11
2	10.22	10.09	10.61	10.30	10.29	10.58
3	10.50	10.29	10.17	10.69	10.64	10.28
4	10.62	10.57	10.12	10.33	10.68	10.45
5	10.69	10.22	10.45	10.09	10.80	10.10
6	10.48	10.24	10.62	10.48	10.11	10.41
7	10.66	10.09	11.03	9.99	10.14	10.28
8	10.09	10.16	10.00	10.18	10.10	10.27
9	10.93	10.71	10.49	10.56	10.12	10.73
10	10.33	10.67	10.57	10.11	10.25	10.30
Average	10.49	10.32	10.45	10.27	10.34	10.35

(e) p = 3 bar

No	E_L of positive (kV/cm)			E_L of negative (kV/cm)		
	Particle 1	Particle 2	Particle 3	Particle 1	Particle 2	Particle 3
1	10.70	11.21	10.95	11.02	10.86	10.89
2	10.69	10.67	10.71	11.23	11.38	10.76
3	11.91	10.87	11.17	10.67	10.66	11.08
4	11.38	11.41	11.02	10.68	10.64	11.35
5	10.82	11.04	10.63	10.82	11.36	10.54
6	11.12	11.86	10.84	10.58	10.62	11.00
7	11.00	10.76	11.41	10.69	10.92	11.26
8	11.20	11.49	11.62	10.64	11.47	10.67
9	10.75	11.14	10.96	10.69	10.83	10.68
10	10.89	12.20	11.22	10.73	10.71	10.75
Average	11.05	11.27	11.06	10.77	10.94	10.90

Table A 4. The stainless steel particle of 1 mm radius liftoff under 1, 2 and 3 bar pressure for the stainless steel ground electrode.

(a) p = 1 bar

No	E_L of positive (kV/cm)			E_L of negative (kV/cm)		
	Particle 1	Particle 2	Particle 3	Particle 1	Particle 2	Particle 3
1	14.85	15.75	15.13	15.36	15.22	15.13
2	15.24	14.91	15.87	14.96	15.02	15.11
3	15.15	14.81	15.04	15.38	15.42	15.08
4	15.20	15.52	15.15	15.29	14.96	15.01
5	15.05	14.96	15.47	15.19	15.12	15.42
6	15.24	14.90	15.12	15.12	15.24	15.50
7	14.97	15.09	15.22	15.30	15.22	15.18
8	15.36	14.82	14.92	15.20	15.10	15.26
9	15.09	15.01	14.81	15.12	15.10	14.90
10	15.06	14.98	15.10	15.05	15.09	15.19
Average	15.12	15.07	15.18	15.20	15.15	15.18

(b) p = 2 bar

No	E_L of positive (kV/cm)			E_L of negative (kV/cm)		
	Particle 1	Particle 2	Particle 3	Particle 1	Particle 2	Particle 3
1	16.29	15.79	15.60	15.80	15.92	16.20
2	15.72	16.55	16.00	15.72	15.70	15.94
3	15.77	15.65	15.78	15.71	16.42	16.34
4	15.70	15.66	15.83	15.67	15.98	16.34
5	15.53	15.79	15.87	15.97	15.98	16.63
6	15.97	16.49	16.34	15.87	15.85	16.26
7	15.67	15.75	16.16	15.68	16.27	16.47
8	15.79	15.85	16.64	15.92	15.98	15.93
9	15.95	16.19	16.16	15.67	15.95	16.33
10	15.78	15.78	16.54	15.93	15.90	16.29
Average	15.82	15.95	16.09	15.79	15.99	16.27

(c) p = 3 bar

No	E_L of positive (kV/cm)			E_L of negative (kV/cm)		
	Particle 1	Particle 2	Particle 3	Particle 1	Particle 2	Particle 3
1	18.06	17.12	16.59	16.38	16.64	16.31
2	17.84	16.35	18.27	16.78	16.75	16.48
3	16.40	16.78	16.35	16.67	16.53	16.84
4	16.88	17.43	16.39	16.69	16.75	16.70
5	15.99	16.09	17.04	17.67	16.36	17.08
6	16.43	17.36	16.06	17.03	16.43	17.11
7	16.84	16.48	16.74	17.65	18.03	16.77
8	17.58	16.70	17.31	17.04	18.11	16.55
9	17.23	18.17	16.60	16.71	16.61	16.61
10	17.18	16.61	18.10	16.39	16.64	16.35
Average	17.04	16.91	16.94	16.90	16.89	16.68

Table A 5. The aluminum particle of 0.4 mm radius liftoff under 1 and 3 bar pressure for the aluminum ground electrode.

(a) p = 1 bar

No	E_L of positive (kV/cm)			E_L of negative (kV/cm)		
	Particle 1	Particle 2	Particle 3	Particle 1	Particle 2	Particle 3
1	6.20	6.02	6.04	6.17	6.24	6.33
2	6.80	6.12	5.86	6.61	5.89	6.51
3	6.67	6.04	6.52	6.03	5.96	5.92
4	6.54	5.90	6.38	6.20	6.54	6.06
5	6.54	6.61	6.22	6.54	6.41	6.55
6	6.06	6.23	6.04	6.48	6.20	6.86
7	6.72	6.43	6.02	6.05	6.19	6.25
8	5.99	6.39	6.50	6.31	6.73	6.61
9	6.26	6.52	6.25	6.73	6.29	6.34
10	6.13	6.52	6.03	5.99	6.15	6.60
Average	6.39	6.28	6.18	6.31	6.26	6.40

(b) p = 3 bar

No	E_L of positive (kV/cm)			E_L of negative (kV/cm)		
	Particle 1	Particle 2	Particle 3	Particle 1	Particle 2	Particle 3
1	7.26	6.62	6.70	6.65	7.28	7.07
2	6.59	6.81	6.48	7.03	6.61	7.16
3	7.95	6.94	6.61	7.37	7.94	7.22
4	6.95	7.21	6.81	7.51	6.72	7.60
5	7.12	6.66	6.80	6.54	8.22	6.65
6	6.52	7.40	6.98	6.47	6.92	6.80
7	6.78	7.26	7.18	6.81	6.72	6.82
8	6.81	7.01	6.66	6.78	6.87	7.99
9	6.79	6.50	6.93	6.52	7.41	6.66
10	7.66	8.36	8.13	7.06	7.01	6.77
Average	7.04	7.08	6.93	6.88	7.17	7.07

Table A 6. The steel particle of 0.5 mm radius liftoff under 1, 2 and 3 bar pressure for the aluminum ground electrode.

(a) p =1 bar

No	E_L of positive (kV/cm)			E_L of negative (kV/cm)		
	Particle 1	Particle 2	Particle 3	Particle 1	Particle 2	Particle 3
1	11.12	10.86	11.23	11.89	11.12	10.93
2	10.73	11.18	12.04	11.20	12.03	11.72
3	11.11	11.10	11.05	11.32	11.10	11.18
4	11.06	10.71	10.86	10.84	11.15	11.13
5	11.10	11.59	11.62	10.77	11.28	11.17
6	10.90	11.08	10.99	11.14	11.41	11.03
7	11.32	10.96	11.53	11.21	11.20	11.33
8	11.40	11.86	10.93	11.05	11.48	11.27
9	10.96	10.96	11.37	11.47	11.39	11.17
10	11.39	11.10	11.00	11.49	10.77	11.45
Average	11.11	11.14	11.26	11.24	11.29	11.24

(b) p =2 bar

No	E_L of positive (kV/cm)			E_L of negative (kV/cm)		
	Particle 1	Particle 2	Particle 3	Particle 1	Particle 2	Particle 3
1	12.24	12.77	11.61	11.15	11.74	11.30
2	12.85	11.35	11.37	12.14	11.69	12.29
3	11.41	12.47	11.18	12.13	11.44	11.97
4	12.08	11.69	11.27	12.57	12.35	12.52
5	11.23	11.28	11.52	11.69	11.49	11.39
6	11.28	11.13	11.65	11.92	11.52	12.33
7	11.27	11.23	12.18	11.38	12.82	11.56
8	12.23	11.38	11.58	12.31	11.63	12.18
9	11.51	11.52	11.45	11.31	12.01	11.39
10	11.41	11.86	12.33	12.49	11.93	11.86
Average	11.75	11.67	11.61	11.91	11.86	11.88

(c) p = 3 bar

No	E_L of positive (kV/cm)			E_L of negative (kV/cm)		
	Particle 1	Particle 2	Particle 3	Particle 1	Particle 2	Particle 3
1	12.57	12.23	12.97	12.82	12.69	12.43
2	12.13	12.11	12.01	12.75	12.64	12.68
3	13.02	12.63	12.00	12.36	13.24	12.44
4	12.71	13.59	12.76	12.68	13.14	12.58
5	12.36	12.41	12.52	12.62	12.70	12.62
6	12.70	12.49	12.81	12.82	13.64	12.84
7	12.83	12.44	12.47	12.24	12.75	12.03
8	12.82	12.24	12.31	12.36	12.84	12.61
9	12.22	12.91	12.57	12.70	13.03	12.61
10	12.42	12.33	12.76	12.69	12.77	12.61
Average	12.58	12.54	12.52	12.60	12.94	12.54

APPENDIX B: The raw data of experimental results for particle liftoff in the air/N_2 mixture.

Table B 1. The aluminum particle of 0.4 mm radius liftoff under 1 and 3 bar pressure for the stainless steel ground electrode.

(a) p = 1 bar

No	E_L of positive (kV/cm)			E_L of negative (kV/cm)		
	Particle 1	Particle 2	Particle 3	Particle 1	Particle 2	Particle 3
1	7.07	6.52	6.89	6.37	6.15	6.27
2	6.77	6.46	6.72	6.22	6.02	6.07
3	6.64	6.31	6.07	6.50	6.74	6.39
4	6.77	6.18	6.40	6.71	6.13	6.02
5	6.48	5.99	6.79	6.53	6.25	6.00
6	6.12	6.05	5.98	5.98	6.43	6.30
7	6.07	6.06	6.22	6.17	6.43	6.41
8	6.26	6.34	6.66	6.02	5.77	6.44
9	6.40	6.98	5.90	6.32	6.27	6.47
10	6.34	5.95	5.89	6.25	5.93	6.11
Average	6.49	6.28	6.35	6.31	6.21	6.25

(b) p = 3 bar

No	E_L of positive (kV/cm)			E_L of negative (kV/cm)		
	Particle 1	Particle 2	Particle 3	Particle 1	Particle 2	Particle 3
1	6.57	7.96	6.77	6.93	6.62	6.81
2	6.65	7.77	6.81	6.93	6.87	6.98
3	6.93	6.94	6.58	6.44	6.79	6.43
4	6.88	6.57	8.23	6.86	7.05	6.54
5	6.64	7.57	6.47	7.85	7.44	6.78
6	7.20	8.22	6.95	6.66	6.78	6.59
7	7.06	6.77	7.56	7.69	6.98	6.99
8	6.85	6.43	6.85	6.89	6.38	6.94
9	6.98	6.47	6.92	7.64	6.77	6.52
10	6.79	6.59	7.23	6.74	6.62	7.15
Average	6.85	7.13	7.04	7.06	6.83	6.77

Table B 2. The aluminum particle of 0.68 mm radius liftoff under 1and 3 bar pressure for the stainless steel ground electrode.

(a) p = 1 bar

No	E_L of positive (kV/cm)			E_L of negative (kV/cm)		
	Particle 1	Particle 2	Particle 3	Particle 1	Particle 2	Particle 3
1	7.58	7.75	7.70	7.22	7.27	7.90
2	7.35	8.05	7.69	8.02	7.46	7.77
3	7.44	7.75	7.40	7.74	7.41	7.42
4	7.35	7.63	7.62	7.57	7.80	7.81
5	7.82	7.58	7.30	7.44	7.57	7.70
6	7.49	8.05	7.51	7.88	7.54	7.96
7	7.77	7.90	7.51	7.76	7.57	7.58
8	7.99	7.46	7.46	7.82	7.81	7.70
9	7.69	7.48	7.62	7.58	7.80	7.81
10	7.81	7.78	7.68	7.57	7.68	7.87
Average	7.63	7.74	7.55	7.66	7.59	7.75

(b) p = 3 bar

No	E_L of positive (kV/cm)			E_L of negative (kV/cm)		
	Particle 1	Particle 2	Particle 3	Particle 1	Particle 2	Particle 3
1	8.86	8.50	8.28	8.69	8.40	8.18
2	8.51	8.18	8.18	8.13	8.99	8.43
3	8.54	8.94	8.71	8.99	8.23	8.10
4	8.51	8.35	9.20	8.24	8.28	8.18
5	8.36	8.35	9.27	9.31	8.56	8.18
6	8.51	8.49	8.46	9.00	8.46	9.19
7	8.37	8.45	8.22	8.45	8.45	8.40
8	8.98	8.29	8.79	8.58	8.50	8.65
9	8.49	8.44	8.11	8.71	8.11	8.58
10	8.85	8.36	8.37	8.40	8.22	8.44
Average	8.60	8.43	8.56	8.65	8.42	8.43

Table B 3. The aluminum particle of 1.19 mm radius liftoff under 1and 3 bar pressure for the stainless steel ground electrode.

(a) p = 1 bar

No	E_L of positive (kV/cm)			E_L of negative (kV/cm)		
	Particle 1	Particle 2	Particle 3	Particle 1	Particle 2	Particle 3
1	9.77	9.75	9.84	10.01	9.97	9.94
2	10.17	9.70	10.08	9.81	9.81	9.91
3	9.90	9.83	10.00	9.98	9.77	10.02
4	9.69	9.66	9.55	9.96	9.67	9.86
5	9.66	9.66	9.61	9.68	9.82	9.73
6	9.70	9.67	9.56	9.53	9.50	9.50
7	9.84	9.73	10.02	9.55	9.70	9.72
8	9.42	9.61	9.50	9.83	9.54	9.80
9	9.62	9.53	9.69	9.70	9.76	9.86
10	9.48	9.45	9.74	9.61	9.97	9.90
Average	9.73	9.66	9.76	9.77	9.75	9.82

(b) p = 3 bar

No	E_L of positive (kV/cm)			E_L of negative (kV/cm)		
	Particle 1	Particle 2	Particle 3	Particle 1	Particle 2	Particle 3
1	11.10	10.85	10.57	10.77	10.67	10.73
2	11.13	10.71	10.78	11.06	10.82	10.92
3	10.71	11.32	10.82	11.33	11.21	11.06
4	10.98	11.05	11.08	11.08	11.04	10.80
5	11.41	10.73	10.73	11.05	10.77	10.71
6	10.94	10.72	10.94	10.83	10.80	10.92
7	10.86	10.79	10.77	10.90	10.76	10.67
8	11.21	10.78	10.89	11.08	10.93	11.06
9	10.78	10.90	11.32	10.92	11.13	11.21
10	10.92	11.25	10.72	11.19	11.17	11.33
Average	11.00	10.91	10.86	11.02	10.93	10.94

APPENDIX C: The raw data of experimental results for particle liftoff in the air/SF_6 mixture.

Table C 1. The aluminum particle of 0.4 mm radius liftoff under 1and 3 bar pressure for the stainless steel ground electrode.

(a) p = 1 bar

No	E_L of positive (kV/cm)			E_L of negative (kV/cm)		
	Particle 1	Particle 2	Particle 3	Particle 1	Particle 2	Particle 3
1	6.51	6.00	6.45	5.99	6.61	5.90
2	5.81	5.84	6.13	6.11	5.83	6.09
3	6.54	6.37	6.04	6.16	6.52	5.96
4	6.15	6.16	5.81	6.59	6.05	6.41
5	5.92	5.91	6.38	6.45	6.18	6.44
6	6.07	6.06	6.22	6.44	6.20	5.84
7	6.05	5.96	5.88	6.34	6.09	6.59
8	5.93	5.97	6.24	5.78	6.11	6.03
9	5.95	5.91	6.24	6.05	6.13	6.07
10	5.90	6.26	6.48	6.03	6.16	6.39
Average	6.08	6.04	6.19	6.19	6.19	6.17

(b) p = 3 bar

No	E_L of positive (kV/cm)			E_L of negative (kV/cm)		
	Particle 1	Particle 2	Particle 3	Particle 1	Particle 2	Particle 3
1	7.05	6.81	7.21	6.86	6.86	6.54
2	6.66	6.41	6.59	6.89	6.75	7.00
3	6.79	6.91	6.77	6.60	7.54	6.72
4	6.99	7.25	7.13	7.33	6.91	6.65
5	6.94	7.25	7.06	6.93	7.00	6.72
6	6.78	6.64	6.72	6.93	6.46	6.41
7	6.81	7.27	7.14	7.27	7.07	7.37
8	6.73	6.99	7.26	6.43	6.71	6.86
9	7.03	7.54	7.18	6.75	7.32	6.40
10	6.98	6.86	7.03	6.81	7.03	6.93
Average	6.88	6.99	7.01	6.88	6.96	6.76

Table C 2. The aluminum particle of 0.68 mm radius liftoff under 1and 3 bar pressure for the stainless steel ground electrode.

(a) p = 1 bar

No	E_L of positive (kV/cm)			E_L of negative (kV/cm)		
	Particle 1	Particle 2	Particle 3	Particle 1	Particle 2	Particle 3
1	7.39	7.67	7.28	7.40	7.33	7.53
2	7.60	7.39	7.62	7.42	7.42	7.53
3	7.71	7.47	7.15	7.47	7.27	7.41
4	7.16	7.81	7.57	7.25	7.43	7.58
5	7.83	7.54	7.43	7.61	7.47	7.62
6	7.16	7.20	7.32	7.34	7.30	7.67
7	7.58	7.15	7.60	7.63	7.40	7.71
8	7.69	7.46	7.56	7.44	7.26	7.33
9	7.35	7.30	7.56	7.22	7.62	7.19
10	7.41	7.42	7.50	7.41	7.53	7.47
Average	7.49	7.44	7.46	7.42	7.40	7.50

(b) p = 3 bar

No	E_L of positive (kV/cm)			E_L of negative (kV/cm)		
	Particle 1	Particle 2	Particle 3	Particle 1	Particle 2	Particle 3
1	8.42	8.59	8.53	8.29	8.24	8.53
2	8.26	8.46	8.43	8.40	8.57	8.58
3	8.40	8.69	8.58	8.39	8.50	8.29
4	8.59	8.80	8.57	8.56	8.60	8.47
5	8.28	8.42	8.45	8.17	8.39	8.56
6	8.72	8.64	8.32	8.18	8.40	8.58
7	8.74	8.61	8.71	8.29	8.43	8.53
8	8.37	8.19	8.21	8.57	8.38	8.38
9	8.38	8.44	8.46	8.72	8.44	8.58
10	8.51	8.85	8.28	8.45	8.80	8.33
Average	8.47	8.57	8.45	8.40	8.48	8.48

Table C 3. The aluminum particle of 1.19 mm radius liftoff under 1and 3 bar pressure for the stainless steel ground electrode.

(a) p = 1 bar

No	E_L of positive (kV/cm)			E_L of negative (kV/cm)		
	Particle 1	Particle 2	Particle 3	Particle 1	Particle 2	Particle 3
1	10.15	9.45	9.59	9.63	9.62	9.94
2	9.69	9.64	9.81	9.69	9.70	9.87
3	9.69	9.74	9.62	9.77	9.89	9.57
4	9.55	10.14	9.56	9.80	9.68	9.62
5	9.67	9.94	9.88	9.81	9.62	9.59
6	9.83	10.12	9.83	9.54	9.89	9.61
7	9.68	9.76	10.00	9.80	9.64	9.67
8	9.55	9.54	9.90	9.47	9.53	9.75
9	9.55	9.94	9.94	9.61	9.79	10.02
10	9.88	9.60	9.87	9.63	9.80	9.81
Average	9.72	9.79	9.80	9.68	9.72	9.74

(b) p = 3 bar

No	E_L of positive (kV/cm)			E_L of negative (kV/cm)		
	Particle 1	Particle 2	Particle 3	Particle 1	Particle 2	Particle 3
1	10.82	11.27	10.93	10.93	10.90	10.90
2	10.91	11.08	11.08	10.86	10.82	10.93
3	10.82	11.17	11.28	11.20	11.11	11.27
4	10.85	10.87	10.98	10.93	10.91	10.85
5	10.98	10.64	10.82	10.71	10.76	10.80
6	10.85	10.86	10.87	10.77	10.87	10.92
7	10.83	10.76	11.10	10.72	10.87	10.91
8	10.85	10.84	10.75	10.89	10.70	10.67
9	10.76	10.75	10.78	10.80	10.72	10.86
10	10.67	11.01	11.17	10.66	10.82	10.79
Average	10.83	10.93	10.98	10.85	10.85	10.89

VITA

Monekham Vilaisien was born in Khammouane, Lao PDR, on 2 September 1985. He received the B. Eng. degree in 2011 from National University of Laos. The article was published as follows:

1.“Study on the effects of gas pressure and particle size on the liftoff of conducting particles,” in 2016 13th International Conference on Electrical Engineering/Electronics, Computer, Telecommunications and Information Technology (ECTI-CON), 2016, pp. 1-5.

2.“Study on the effects of gas pressure on the liftoff of conducting particles in different gas media,” in 2016 18th Asian Conference on Electrical Discharge (ACED 2016).